HHS Public Access

Author manuscript

Reprod Toxicol. Author manuscript; available in PMC 2017 August 01.

Published in final edited form as:

Reprod Toxicol. 2016 August ; 63: 32–48. doi:10.1016/j.reprotox.2016.03.042.

Mono-2-ethylhexyl phthalate disrupts neurulation and modifies the embryonic redox environment and gene expression

Karilyn E. Sant[a], **Dana C. Dolinoy**[a,b], **Joseph L. Jilek**[a], **Maureen A. Sartor**[c,d], and **Craig Harris**[a,b]

[a]Department of Environmental Health Sciences, University of Michigan School of Public Health, Ann Arbor, MI 48109

[b]Department of Nutritional Sciences, University of Michigan School of Public Health, Ann Arbor, MI 48109

[c]Department of Computational Medicine & Bioinformatics, University of Michigan Medical School, Ann Arbor, MI 48109

[d]Department of Biostatistics, University of Michigan School of Public Health, Ann Arbor, MI 48109

Abstract

Mono-2-ethylhexl phthalate (MEHP) is the primary metabolite of di-2-ethylhexyl phthalate (DEHP), a ubiquitous contaminant in plastics. This study sought to determine how structural defects caused by MEHP in mouse whole embryo culture were related to temporal and spatial patterns of redox state and gene expression. MEHP reduced morphology scores along with increased incidence of neural tube defects. Glutathione (GSH) and cysteine (Cys) concentrations fluctuated spatially and temporally in embryo (EMB) and visceral yolk sac (VYS) across the 24h culture. Redox potentials (E_h) for GSSG/GSH were increased by MEHP in EMB (12h) but not in VYS. CySS/CyS E_h in EMB and VYS were significantly increased at 3h and 24h, respectively. Gene expression at 6h showed that MEHP induced selective alterations in EMB and VYS for oxidative phosphorylation and energy metabolism pathways. Overall, MEHP affects neurulation, alters E_h, and spatially alters the expression of metabolic genes in the early organogenesis-stage mouse conceptus.

Keywords

embryo; neural tube defects; MEHP; DEHP; visceral yolk sac; redox potential; glutathione; cysteine; gene expression

Corresponding Author: charris@umich.edu, Phone: +1 (734) 936-3397, Department of Environmental Health Sciences, University of Michigan, School of Public Health, M6108 SPH II, 1415 Washington Heights, Ann Arbor MI 48109-2029.

1. Introduction

Development is a highly regulated process that relies on tightly controlled intra- and intercellular signaling for normal growth. Dysregulation of embryogenesis can be caused by a myriad of genetic, physiological, and environmental factors such as the chemicals found in our air, water, and food. Exposure to chemical agents can alter specific signaling pathways to manipulate cell polarity and migration, membrane transport, and protein structure and function [1–4]. Ultimately, these changes can manifest as spontaneous abortions, birth defects, and growth deficits or predispose individuals to diseases that arise during childhood and into adulthood. One such factor that can lead to this dysregulation is altered redox signaling and control, caused by perturbations of the soluble thiol steady state, along with an increase in reactive oxygen species (ROS) [5]. Many human and animal teratogens, compounds that produce congenital malformations, are reported to act through classical oxidative stress: a change from a balanced and reducing intracellular redox environment to predominantly oxidizing conditions, concurrent with the generation of ROS [6]. An oxidizing environment during development has also been associated with increased risk of postnatal chronic diseases including neurodegeneration, hypertension, cancer, and Type II Diabetes [7–9]. Environmental contaminants, including the phthalates discussed in this report, have also been shown to increase the generation of ROS [10–13]. Views about the roles of increased ROS generation in biological cells and tissues have changed of late because ROS are now known to have critical signaling and regulatory roles in normal cell function [14–16]. These discoveries have helped dispell the previous notion that all ROS are deleterious. Through the selective oxidation and reduction of protein thiols, critical cell processes such as enzyme activity, receptors, transporters, transcription factors, and second messenger signaling are all regulated. While related, the widespread practice of invoking “oxidative stress” through the simple measurement of glutathione (GSH) depletion or increases in markers of lipid peroxidation because they vary naturally and do not represent the significance of the broader redox environment [17]. Many of the regulatory consequences of altered redox status have been more accurately assessed by measuring intracellular redox potentials (E_h). which, although based on the GSSG/GSH redox couples, are a more sensitive indicator of environmentally-induced perturbations to the redox steady state. Progressive increases in intracellular E_h are highly correlated with changes in proliferation, differentiation, and tissue patterning during embryogenesis and organogenesis [5, 18]. Altered E_h during embryonic development can range from mild to severe, leading to manifestations ranging from distorted signal transduction to apoptosis and necrosis, respectively. Because these consequences are likely harmful, the body has an endogenous and dynamic antioxidant system to prevent and protect against the more damaging consequences of oxidation. The reducing agent glutathione (GSH) and related enzymes glutathione reductase, glutathione peroxidase, and glutamate-cysteine ligase are primarily responsible for the maintenance of a balanced cellular E_h [17]. Production and recycling of these endogenous antioxidants is regulated through the induction of the Nrf2 antioxidant pathway [19]. The action of other redox couples, such as reduced cysteine (Cys) and oxidized cysteine (CySS) or thioredoxin, help maintain steady redox states and govern redox signaling in the embryo. When the actions of all of these antioxidants and protective

enzymes are insufficient to maintain a balanced environment during development, teratogenesis can occur [5].

Mono-2-ethylhexyl phthalate (MEHP) is the primary metabolite of the common plasticizing agent, di-2-ethylhexyl phthalate (DEHP). DEHP has been widely incorporated into many products worldwide, but is of special concern because of its inclusion in vinyl piping and medical tubing. Evidence of phthalate transfer to the EMB and fetus has been evident through detection of MEHP in meconium, amniotic fluid, cord blood, rodent fetal tissues, and placental perfusate [20–28]. It has been previously demonstrated that MEHP can induce general oxidative stress and inflammation in various reproductive tissues and developmental tissues via the increased generation of ROS, though these studies were conducted in other model organisms and at different stages of development [12, 13, 29, 30]. It has been demonstrated that several chemical compounds have the ability to modify the embryonic redox environment, and that these changes can result in teratogenic outcomes [5, 31–35]. Compounds such as ethanol, diamide, methylmercury, phenytoin, and L-buthionine-S,R-sulfoximine have been associated with oxidation of the various tissue and fluid compartments of the conceptus, including VYS, the yolk sac fluid (YSF), amniotic fluid (AF), and the EMB [34, 36–38]. These compounds are able to decrease GSH concentrations and selectively increase Eh in conceptal tissues and fluids. The body of evidence for other toxicants altering redox signaling in the organogenesis-stage conceptus is growing, and many of these exposures are associated with adverse health outcomes and structural defects.

Thus, it was important to determine the ontogeny of E_h across the susceptible window of early organogenesis in order to identify potential windows of susceptibility for phthalate exposure and relate disturbances to sensitive developmental events. The goals of this study were to characterize MEHP-induced morphology and growth changes in mouse whole embryo culture (mWEC), determine whether MEHP alters conceptal E_h inEMB and VYS tissues, and to identify related MEHP-induced changes in gene expression.

2. Materials & Methods

2.1 Chemicals and reagents

Mono-2-ethylhexyl phthalate was obtained from AccuStandard (New Haven, CT). Dioctyl phthalate (DEHP), dimethyl sulfoxide (DMSO), glutathione, glutathione disulfide, cysteine, cystine, γ-glutamyl-glutamate, iodoacetic acid, iodoacetamide, bicinchoninic acid, RNAlater®, Tyrode's balanced salt solution, and penicillin/streptomycin (10,000 units/ml penicillin, 10,000 μg/ml streptomycin sulfate) were obtained from Sigma/Aldrich (St. Louis, MO). Hanks balanced salt solution (HBSS) was purchased from GIBCO/Life Technologies (Grand Island, NY). Dansyl chloride was purchased from Fluka Chemie/Sigma-Aldrich (St. Louis, MO). Glacial acetic acid was obtained from Fisher Scientific (Waltham, MA).

2.2 Mouse whole embryo culture

Mouse embryo culture was performed according to the procedures outlined in [39]. Briefly, female CD-1 mice were time-mated and obtained from Charles River (Portage, MI). The morning of discovery of a vaginal plug was designated as gestational day (GD) 0. Animals

were maintained on a 12h light-12h dark cycle and were supplied food and water *ad libitum*. On GD 8, female mice were euthanized with CO_2 (10–30%) and the uterus was removed. Culture-ready conceptuses (ranging from 6–8 somites) were explanted from the uterus, removed from the decidual mass, freed from the Reichert's membrane, randomized, and placed into 10 ml culture bottles containing 5 ml of 75% heat-inactivated rat serum/25% Tyrode's balanced salt solution (TBSS) and 21.5 μl penicillin/streptomycin. Immediately centrifuged rat serum was collected and prepared from female Sprague Dawley rats according to approved protocols [39]. The number of conceptuses per bottle never exceeded the standard rule of 1 conceptus per ml of culture medium. Bottles were placed on a continuous-gassing carousel in an incubator held at 37°C and supplied with 5% O_2/5% CO_2/90% N_2. After 6 h in culture, the gas input was changed to 20% O_2/5% CO_2/75% N_2 to optimize growth in culture. All animal procedures were approved by the University of Michigan University Committee on Use and Care of Animals.

2.3 Exposure and sample collection

DEHP and MEHP were suspended in DMSO to increase solubility in culture. DEHP and MEHP were added to the culture medium to bring the final concentration in culture to 100, 250, 500, or 1000 μg/ml (0.4–3.6 mM MEHP and 0.3–2.6 mM DEHP). These concentrations were selected based upon concentrations utilized in other phthalate whole embryo culture studies [40, 41]. WEC experiments, like cell culture experiments, frequently use concentrations greater than those observed *in vivo* due to the lack of direct perfusion to the tissues, and thus these concentrations are 1–3 orders of magnitude greater than those observed in human cord blood [27, 28]. DMSO was added to control bottles at a concentration of 0.05% (v/v) in culture, equal to the volume of added DEHP and MEHP solutions. For morphology experiments, conceptuses were grown in culture for a total of 24 h before removal. For redox analysis, conceptuses were sampled at 0 h (before explant into culture), and at 1, 3, 6, 12, and 24 h of culture. Samples designated for RNA isolation were collected following 6 h in culture. At the time of removal from culture, all conceptuses were washed 2X in Hank's balanced salt solution (HBSS) and ectoplacental cones were removed. The EMB and VYS were manually separated using watchmaker's forceps. At this time, samples were either designated for morphology assessment or for redox analysis. Individual (unpooled) samples for redox analysis were placed into thiol preservation buffer (containing 5% perchloric acid, 0.2 M boric acid, and 10 μM γ-glutamylglutamate), snap frozen in liquid N_2, and stored at −76° C, as specified in [18]. Tissues collected for RNA isolation were pooled (n=5 per sample) and placed into RNA later and stored at −76° C.

2.4 Morphology Assessment

At the conclusion of the culture period, conceptuses for morphology assessment were removed from culture and washed thoroughly in HBSS without disruption. Once rinsed, conceptuses were transferred into a dish containing fresh HBSS for microscopic analysis. Images were taken before and after removal of the VYS on a stage micrometer-calibrated microscope, and all were imaged at the same magnification. Morphological parameters were evaluated as specified in [39]. In short, we evaluated quality and developmental progress of the VYS, allantois, heart, flexion, caudal neural tube, forebrain, midbrain, hindbrain, otic vesicle, optic cups, forelimbs, mandible, maxillary process, and counted the number of

somite pairs. Additionally, crown-rump length, VYS diameter, and head length were measured [39]. VYS volume was calculated by applying the average radius length to the formula for spherical volume ($4/3\pi r^3$). Protein quantification of tissue was done using bicinchoninic acid (BCA) assay on a microplate reader [42].

2.5 HPLC analysis of thiols and redox potentials

Samples were thawed on ice and prepared for HPLC analysis of soluble thiols as previously described in [36, 43]. Briefly, a Waters 2695 Alliance Separations module equipped with a Supelcosil LC-NH_2 column (Sigma, St. Louis, MO) was coupled with a Waters 2475 Fluorescence Detector. Reverse-phase chromatography was used to measure reduced glutathione (GSH), oxidized glutathione disulfide (GSSG), reduced cysteine (Cys), and oxidized cystine (CySS). Flow was set to 1 mL/min using a mobile phase gradient consisting of mobile phase A consisting of 80% methanol and mobile phase B consisting of 62.5% methanol, 12.5% glacial acetic acid, and 214 mg/ml sodium acetate trihydrate. Peaks were visualized by fluorescence detection (excitation 335 nm, emission 518 nm) and peaks were processed using the Waters Empower software (Milford, MA). The Nernst equation (pH 7.4) was used for the calculation of E_h for both the Cys/CySS and GSH/GSSG redox pairs: $E_h = -264+30 \log([GSSG]/[GSH]^2)$, Cys/CySS, $E_h = -250+30 \log([CySS]/[Cys]^2)$ as described previously [18]. Absolute concentrations of GSH, GSSG, Cys, and CySS were calculated and normalized to tissue protein concentrations determined by BCA assay.

2.6 RNA isolation and Affymetrix microarray analysis of expression

VYS and EMB samples collected from M100 conceptuses at the 6 h mark on GD8 and stored in RNAlater (Fisher Scientific) were thawed on ice and RNA was isolated following the instructions of the RNeasy Mini Kit (Qiagen). The 6 h time point was selected because it is a sensitive period of development, during which organogenesis of several major organs has begun. Additionally, this time point allowed for us to assess the acute effects of MEHP exposure while avoiding expression changes merely induced by the initial stress of the culture environment. RNA (n=3 for each treatment, for each tissue) was submitted for Affymetrix microarray processing at the University of Michigan Microarray Core Facility. Mouse MG-430 PM strip arrays were processed using the IVT Express Kit (Affymetrix). RNA purity and integrity were confirmed using the RNA 6000 Nano Kit for the Agilent 2100 Bioanalyzer. Raw data obtained for the array was further examined for quality and supported by satisfactory scores for PM chip density, RNA degradation, and standard errors. Robust multi-array average (RMA) was used for background correction, normalization, and quantification of $\log_2$ expression using default parameters in R v2.4.1. Principle component analysis revealed distinctions between sample groups, confirming EMB and VYS tissue differences (Supplementary Figure 1).

Overall differences in expression between control and MEHP-treated EMB and VYS were examined using the *Limma* package in R 2.4.1. The *lmFit* function was used to downweight potential outliers, and *eBayes* was used to calculate p-values and FDR levels using an empirical Bayesian moderated t-test and the Benjamini and Hochberg adjustment for multiple testing [44]. Validation of gene expression results was done by performing quantitative PCR on selected candidate genes. Enrichment of gene sets was analyzed using

LRpath, and biologically and statistically altered processes and pathways were identified using the GO Biological Processes (http://geneontology.org/) and KEGG Pathway (http://www.genome.jp/kegg/) databases [45]. Pathways containing genes with many statistical differences between control and MEHP-treated tissues were considered “enriched”.

2.7 Statistical Analysis

Values presented in this paper are means ± standard error of the mean. Statistical outliers were removed, identified as values 1.5 times the interquartile range outside of the first and third quartiles of the data. One-way ANOVA with Tukey posthoc tests and independent t-tests were used to assess statistical significance of differences between groups of data. A confidence level of 95% was used, and p-values <0.05 were deemed as statistically significant changes.

3. Results

3.1 Morphology Assessment

After 24h of culture, phthalate-treated conceptuses were examined for changes in growth and anatomical outcomes using both the parent compound (DEHP) and the metabolite (MEHP) and compared using our standard morphology scoring protocol [39]. Conceptuses in mWEC were exposed, beginning on GD 8 (0h), to DEHP at concentrations of 100 μg/ml (D100), 500 μg/ml (D500), or 1000 μg/ml (D1000); or to MEHP at concentrations of 100 μg/ml (M100), 250 μg/ml (M250), 500 μg/ml (M500), or 1000 μg/ml (M1000). Concentrations were selected based upon benchmark concentrations obtained from other studies [40], and were deemed to be appropriate based on the results of this study [41]. Conceptuses treated with MEHP uniformly exhibited morphological changes, while conceptuses treated with DEHP did not show any growth deficits or malformations (Fig. 1). This is consistent with the understanding that DEHP is metabolized maternally prior to conceptal exposure, and that MEHP is the active metabolite that can cause developmental defects. Conceptuses treated with MEHP were noticeably smaller than controls, and overall size decreased in a dose-dependent fashion (Fig. 2). Table 1 displays the average scores for all morphological parameters after MEHP treatment. Control conceptuses (n=17) had an average total morphology score of 86.6 ± 6.1. None had any defects, and growth parameters were consistent with those observed in other mWEC experiments. Treatment significantly reduced many of the scores, though it seemed to have had little effect on the mandibular or forelimb parameters. Of the most commonly affected developmental outcomes, incomplete closure of the neural tube (neural tube defect) was the prominent feature. Neural tube closure was significantly delayed by MEHP treatment in the cephalic fore-, mid-, and hindbrain segments as well as in the caudal neuropore (Fig. 3).

3.2 MEHP morphology

The M100 group (n=7) had an average total morphology score of 73.8 ± 3.8. Twenty nine percent of M100 embryos exhibited hypoplastic forebrain regions, and 43% of the embryos had open neural tubes at least at one of the four neural tube regions examined (forebrain, midbrain, hindbrain, caudal neural tube). One of the seven MEHP-treated embryos developed a clear blister on the prosencephalon.

The M250 (n=6) had an average total morphology score of 72.9 ± 2.9. All but one of the embryos had an open neural tube at one or more of the neural tube regions scored. Though all of the caudal neural tubes were closed in the M250 group, all structures were highly hypoplastic at this locus.

The M500 (n=16) group had an average morphology score of 56.6 ± 3.3, indicating a significant decrease in overall growth and an increase in anatomical lesions. Hypoplasia of the caudal neural tube was prominent. About a third of the embryos possessed caudal neural tubes that were so necrotic that they could not be fully assessed as to the status of the caudal neuropore. In all of the embryos, the caudal region was truncated, hypoplastic, and presented with a 'zig-zag' pattern running along the dorsal ridge. One of the embryos had complete dissociation of the neural epithelium, with large blisters and severe hypoplasia in the forebrain region. In approximately one-third of the M500 embryos, the pericardium was enlarged and fluid-filled, and these same embryos had blood pooling in the antimesometrial end of the VYS. One of the M500 embryos also had a very thin second branchial arch.

The M1000 group (n=7) was the first exposure that resulted in loss of viability in some of the conceptuses, with an average morphology score of 28.4 ± 0.8. Two of the seven embryos examined were not viable (lacked a heartbeat) and were excluded from the morphological assessment; those that survived had very weak heartbeats in terms of rate and apparent contractile force. All of the M1000 embryos were hypoplastic at the caudal end, and had the 'zig-zag' pattern running along the dorsal ridge. All lacked a posterior neuropore, had blood pooling in the antimesometrial end of the VYS, thin second branchial arches, and signs of necrosis. In one of these embryos, necrotic debris was visible within the hindbrain region.

3.3 DEHP morphology

Compared to the MEHP-treated conceptuses, the DEHP-treated conceptuses (n=5 for each group) were normal morphologically. All groups were morphologically similar to controls without loss of viability, and therefore only gross morphological scores are shown (Figure 1). Due to the lack of apparent toxicity no other detailed information on DEHP was included in this report.

3.4 Soluble Thiol Concentrations in VYS and EMB

In order to illustrate the difficulties in using soluble thiol concentrations as the sole indicator of redox status and the importance of using E_h as an acceptable measure of the perturbations of the intracellular redox steady states, it is necessary to show how variable the oxidized and reduced proportions of the GSSG/GSH and CySS/CyS are within their respective redox couples and how dynamically they change both temporally and spatially over time.

3.4.1 GSH and GSSG—Concentrations (μM) of reduced GSH, and its oxidized counterpart, glutathione disulfide (GSSG), in EMB and VYS (Figure 4) are shown for controls, 100 μM MEHP and 250 μM MEHP treatments sampled at 1, 3, 6, 12 and 24 h of mWEC culture. Qualitative comparisons between EMB and VYS at any given time point show that reduced: oxidized ratios can vary considerably, even across control conceptuses. In this analysis VYS is shown to maintain a greater proportion of GSH in the GSSG form,

implying a greater degree of overall oxidation in this tissue. Depletion of GSH and GSSG caused by MEHP treatment occurs primarily at 1h and 12 h in the EMB and at 12 h in the VYS. In cases where a significant depletion of GSH occurs due to phthalate exposure, it is of interest to note that GSSG does not usually increase as might be expected. By 24h of culture, both EMB and VYS have resolved earlier fluctuations between reduced and oxidized species and established a stable and reduced intracellular environment.

3.4.2 CyS and CySS—Cysteine concentrations remain relatively reduced at 1 h in EMB and VYS but then become variably more oxidized over the 3 h and 6 h time points. In the VYS, the greatest oxidation occurs at 6 h and with an optimal combined overall depletion at 6 h. Similar to the GSH and GSSG data shown in Figure 4, MEHP causes overall depletion without a significant shift in CyS/CySS ratios. Intracellular steady state CyS concentrations are known to be regulated dynamically, as CyS and CySS are shuttled between intracellular and extracellular sources [46]. We were unable to measure extracellular concentrations and their dynamic flux in this analysis.

3.5 Total glutathione and cysteine concentrations

Total glutathione and cysteine concentrations are shown for the EMB and VYS (Fig. 6). Total glutathione is defined as the sum of the reduced fraction concentration plus two times the disulfide fraction concentration. Control total GSH concentrations peaked at 1 h in VYS and EMB, increasing by 75% and 90% from the 0 h value, respectively. EMB control concentrations decreased from the 1 h point across the remainder of the culture period, with only a slight increase at 12 h, ending at 24 h at concentrations slightly below the 0 h starting concentrations. Control patterns in the VYS were somewhat different from the EMB where concentrations peaked at 1 h declined at 3 h, and peaked again at 12 h before they also dropped below 0 h control values at 24 h. In MEHP conceptuses, treatment prevented the GSH concentration spike at 1 h in the EMB ($p=0.002$) in both M100 and M250 concentration groups. M100 total GSH concentration peaked at 3 h, and was elevated compared to the dwindling control ($p=0.073$) and M250 ($p<0.001$) total GSH measures. At 12 h, total GSH in the EMB decreased in a dose-dependent manner compared to controls (M100: $p=0.035$; M250: $p<0.001$). However, all embryonic total GSH concentrations were almost identical after 24 h exposures. Embryonic total Cys measures also followed a dose-dependent pattern over the first 6 h of exposure on GD8 but are, however, not significant due to high variability between samples.

3.7 Redox Potentials

Control E_h determinations at the 24 h time point are concordant with values reported from similar developmental stages in other rodent *in vivo* and WEC studies [36, 38, 47]. After 6 h in culture (GD8), EMB GSH/GSSG E_h were chemically reduced in an apparent dose-dependent manner, though these observations were not statistically significant (Fig. 7). After 12 h, MEHP-treated EMB were significantly more oxidized than control EMB, in a dose-dependent manner (M100 $p=0.009$; M250 $p<0.001$). Control EMB GSH/GSSG E_h were -176.9 ± 1.6 mV, and the M100 and M250 groups were -158.3 ± 1.4 and -138.2 ± 4.5 mV, respectively. After 24 h, all samples were much more chemically reduced than at previous time points, likely due to a greater capacity for new GSH biosynthesis. Despite this overall

reduction of E_h in both tissues, a dose-dependent oxidation in the EMB is still apparent. In the VYS, GSH/GSSG E_h at 3 h were more reduced with increasing doses of 100 and 250 μg/ml MEHP (p=0.06 and p=0.04, respectively). These 3 h E_h were −145.4 ± 4.9, −162.2 ± 5.2, −164.5 ± 1.1 mV for control, M100 and M250 groups, respectively. After 24 h, GSH/GSSG E_h were similar across treatment groups.

In the EMB, Cys/CySS E_h was reduced by MEHP treatments after 1 h, though only the 100 μg/ml induced a significant change (p=0.014). After 3 h, EMB were oxidized by MEHP in a dose-dependent fashion though only the 250 μg/ml dose was statistically oxidized compared to controls (p=0.009). EMB CyS E_h were similar for all groups at 12 h, and only the 250 μg/ml EMB were significantly oxidized at 24 h compared to controls (p=0.040). The MEHP-treated VYS Cys/CySS E_h were reduced at the 3 h time point, though the 100 μg/ml MEHP-treated VYS were most significantly reduced (p=0.014). At 12 h, increasing the dose of MEHP appeared to oxidize the VYS, though it was not statistically significant. At the 24 h time point, the controls and 250 μg/ml MEHP-treated VYS had similar E_h, but the 100 μg/ml MEHP-treated VYS were significantly oxidized after 24 h (p<0.001).

3.8 Microarray analysis

MEHP-induced alterations to gene expression profiles in M100 EMB and VYS were examined after 6 h (GD8). In the VYS, 640 probes (1.4%), corresponding to 512 genes, showed an indication of differential expression (p<0.01) by 6 h MEHP treatment. Of these probes, 249 (38.9%) were downregulated and 391 (61.1%) were upregulated. In the EMB, the expression of 1,485 probes (3.3%), corresponding to 1,170 genes, showed an indication of differential expression. Of these probes, 541 (36.4%) were downregulated and 945 (63.6%) were upregulated. Of the genes listed above, 201 were common to both the EMB and VYS.

3.9 KEGG Pathways enriched by MEHP treatment

KEGG pathways significantly enriched by 6 h MEHP treatment in the EMB and VYS are shown in Table 2. “Enriched” pathways are those that contain many significantly changed genes. Several similarities were noted in EMB and VYS in response to MEHP. The most significantly enriched pathway in both EMB and VYS was *oxidative phosphorylation* (p≤0.001). Expression of several NADH dehydrogenase genes was significantly decreased, including *Ndufa3, Ndufs5, Ndufa6*, and especially *Ndufa7* in both EMB and VYS. In EMB, expression of several ATPases and ATP synthases was also significantly altered by MEHP treatment—primarily those of lysosomal and mitochondrial origin. ATPases were primarily upregulated, while ATP synthases were primarily downregulated. Expression of *Uqcr11*, part of the ubiquinol-cytochrome c reductase complex crucial for cellular respiration, was increased in the VYS but decreased in the EMB.

The majority of enriched pathways in both tissues were, in general, metabolic pathways, namely xenobiotic response and amino acid metabolic pathways. The *drug metabolism - cytochrome P450 (CYP450)* and the *glutathione metabolism* pathways were significantly enriched in the VYS as well. Expression of the constituents of these pathways, consisting mostly of CYP450 isozymes, glutathione-S-transferases, and glutathione peroxidases was

significantly increased. Amino acid metabolic pathways including *histidine metabolism*, *arginine and proline metabolism*, and *alanine, aspartate and glutamate metabolism* were all enriched in both EMB and VYS. Starch and sucrose metabolism was also enriched in the EMB.

Retinol metabolism was enriched in the EMB, namely with regards to non-optic pathways. Though involved in the metabolism of Vitamin A, many of the genes most affected by MEHP treatment were involved in the xenobiotic response and direct signal transduction during embryogenesis. Retinol dehydrogenase 1 (Rdh1), the enzyme responsible for the rate-limiting step of retinaldehyde biosynthesis, was significantly decreased in the EMB following MEHP treatment. As previously mentioned, several CYP450 genes were upregulated by treatment—including CYP26 family variants. The function of the CYP26 family is necessary to convert retinaldehyde into retinoic acid, and is essential for guiding posterior tissue patterning by directing Hox genes for hindbrain formation. Interestingly, Hox gene expression was significantly reduced for several Hoxb, Hoxc, and Hoxd variants.

A fraction (1.2%) of affected genes were members of the solute carrier (SLC) gene families, which are evolutionarily well-conserved across the animal kingdom [48] (Table 3). Although no single family was specifically altered in the pathway analysis, the collective volume of significantly altered SLC genes was notable. Though SLCs have a diverse array of functions, all are involved in the transport of important cellular substrates across cellular membranes [49]. The largest group of transporters significantly impacted by MEHP treatment was involved in the mitochondrial transport of solutes. These mitochondrial transporters are important for metabolism, namely in oxidative processes [50]. Expression of *Slc7a9*, involved in CySS absorption and Cys/CySS redox balance, was significantly decreased in EMB [51]. Significant expression changes to members of the SLC6 family, involved in neurotransmission, appear only in the EMB tissue. Decreased expression was observed in several of these genes, crucial for glycine, noradrenaline, and methionine homeostasis. Several patterns were observed in the overall expression of these genes. Though there was a mixture or upregulated and downregulated SLC family expression in the EMB, there was a strong pattern of downregulation in the VYS.

3.10 GO Biological Processes altered by MEHP treatment

GO Biological Processes significantly up- or down-regulated by MEHP exposure for the EMB and VYS are shown in Figure 8. A p-value of less than 0.05 was used to identify significantly changed GO Biological Processes in order to enrich a large number of processes to observe directional trends in related processes. The number of processes significantly changed by MEHP treatment in the EMB, VYS, or both tissues is shown (Fig. 8A). In all, 527 GO Biological Processes were significantly impacted in the EMB, 389 were specific to the VYS, and another 167 were significantly changed in both tissues.

To identify whether the EMB and VYS tissues responded differently to MEHP treatment, the 167 Biological Processes significantly affected in both the EMB and VYS were plotted (Fig. 8B). Processes were grouped by their parent process (metabolic process, etc.) in order to visually detect patterns of altered regulation. The direction and magnitude of change in the VYS is shown on the x-axis, and for the EMB on the y-axis. The majority of processes

were downregulated in the VYS and upregulated in the EMB, and very few processes were downregulated in both tissues. Several processes, or clusters of related processes, had high magnitudes of change in both tissues, and are labeled on the plot accordingly. *Vitamin transport* is one of the most significantly altered processes, and is one of two processes significantly downregulated in both tissues. Two of the most significantly altered genes within this pathway were the *Folr1*, the primary folate receptor, and *Ttpa*, a transporter for Vitamin E. *Oxidative phosphorylation*, *electron transport chain*, and related processes all clustered together, significantly upregulated in the VYS and downregulated in the EMB. Another cluster of developmental processes related to kidney morphogenesis were significantly upregulated in both the EMB and VYS. Most of the processes related to cellular translation are downregulated in the VYS and upregulated in the EMB by MEHP, namely *Amino acid activation*. Interestingly, most processes pertaining to response to stimuli were clustered in the lower-right quadrant, correlated with the expected upregulation in the VYS, but were downregulation in the EMB.

4. Discussion

Development is a tightly regulated process that is governed by integrated signaling pathways and influenced by combinations of genetic and environmental cues. The environmental cues come from a myriad of sources, including toxicant exposures, nutrient availability, disease, maternal hormones, extracellular ligands, altered redox environments and physical stressors. The specific pathways that are altered by environmental toxicants, such as MEHP, have not been well characterized during mammalian organogenesis. In this study, we sought to better understand the correlative spatial and temporal relationships between exposure, growth and anatomical malformations, changes in redox status, and altered gene expression during embryogenesis using the mWEC system.

By way of comparison, the stage of development studied in this report coincides with the early first trimester of human gestation, during active neural tube closure but prior to the establishment to active placental oxygen and nutrient exchange [52, 53]. This study design allowed us to compare structural, biochemical, and regulatory consequences of MEHP exposure independently in the EMB and VYS across a significant 24h time span that brackets the developmental period during which the embryo undergoes axial rotation, closure of the anterior neural tube, initiation of an active heartbeat, vitelline circulation, and onset of forelimb development [54–56]. Assessment of changes to these developmental milestones was made using our standard morphology assessment [39] which is summarized in Table 1 and depicted in Figure 2. Results revealed an MEHP-induced decline in conceptal growth and a significantly elevated incidence of abnormally open neural tubes (NTDs) over the 24h period from GD8 to GD 9. By mouse GD 9, the anterior neural tube should be fully closed while the posterior neuropore remains open as a pin hole while the trunk continues to elongate. The incidence of defectively open neural tubes was significantly increased in culture beginning at the lowest MEHP concentration tested (100μg/ml). The sensitivity of CD-1 mouse conceptuses used in this study was found to be much greater than rat conceptuses grown in WEC during the same relative stage of development [41]. Robinson et al similarly observed abnormal neurulation in rat conceptuses, but only after MEHP concentrations exceeded 600 μg/ml [57]. In spite of a different degree of sensitivity to

MEHP and obvious differences in culture conditions including: a different species (Wistar rat instead of our CD-1 mouse), timing, stage of embryos at initiation of exposure (1–5 somites instead of our 8–10 somites), O_2 gassing protocol, and duration of exposure (48 h instead of our 24 h), the overall morphological and growth outcomes were quite similar to those we observed in mice. While incomplete neural tube closure was the most prominent morphological defect, parameters indicative of overall growth reductions were also prominent in the treatment-related decrease in total morphology scores (Table 1, Figure 1).

Our conclusion that MEHP is a developmental toxicant/teratogen has also been supported by several other studies which have examined effects during different phases of prenatal development. Fairbairn et al observed that zebrafish embryos exposed to dibutyl phthalate during embryogenesis had disrupted axial growth, resulting in severe dysmorphogenesis from incomplete epiboly [58]. Janer et al investigated the consequences of MEHP-treatment in rat whole embryo culture, and found that MEHP treatment in culture significantly reduced overall growth [40]. Species-specific sensitivity to MEHP is not unexpected because similar differences have been observed for many chemical compounds and across several species of conceptus in WEC (reviewed in [59]). Robinson et al investigated the teratogenic and gene expression consequences of congruent MEHP exposures in the EMB only, and at a later time point [41]. Here, we add a novel conceptal tissue comparison for gene expression, at an earlier, and presumably more sensitive, time point during organogenesis.

Several known teratogens have been suggested to exert their embryotoxic effects through the excess generation of reactive oxygen species (ROS), an identity shared with MEHP [5, 10, 11, 13, 60, 61]. Previous studies have demonstrated that phthalates, including MEHP, are capable of inducing oxidizing conditions in the developing embryo, although sampling occurred at different developmental time points and were assessed in different model systems than employed here. Chu et al found increased ROS concentrations in early preimplantation embryos exposed to concentrations of MEHP that were similar to those used in this study [29] as well as to mono-butyl phthalate [62]. Increased ROS were also detected in phthalate-exposed zebrafish eleutherolarvae [63].

The meaningful assessment of chemically-altered redox states in relation to actual effects on biological outcomes is difficult to make due to the inability to account for subtle spatial and temporal changes in redox states, as well as the lack of a defining quantitative endpoint for evaluation of redox-related toxicity. In this study we have chosen to use the estimation of intracellular redox potentials (E_h) as a readout for chemically-induced perturbation of the redox steady state in conceptuses [47]. Maintenance of a proper redox environment has been shown to be crucial for the developmental determination of cell fates. Oxidation of specific protein thiol residues, act as sensitive “on/off” switches for regulating numerous signaling pathways that are influenced by disruption of the redox steady state, often irrespective of changes in the magnitude of total GSH or total CyS concentrations. The consequences of increasing (oxidizing) E_h values have been extensively studied of late and are known to progressively direct cell fate towards proliferation, differentiation, apoptosis, and, eventually, necrosis [61, 64]. Typically, the more reducing environments are correlated with cells undergoing proliferation, while more oxidative environments are associated with differentiation or ultimately, cell death. For related reasons, the protein thiol oxidation

elicited as a result of increased ROS production and the other factors that disturb E_h have also been implicated in controlling the pluripotency of stem cells, which can occur in the formation of cancers [65–68], and which has been implicated in mechanisms leading to anatomical birth defects [5, 61, 69]. Based on a growing body of evidence an E_h shift of +20 mV (GSH/GSSG redox couple) is sufficient to alter cell activity, moving from proliferation to differentiation.; A 50 mV increase creates conditions that can lead to death [70]. At the 12 h time point in WEC, conceptuses exposed to 100 or 250 μg/ml MEHP resulted in Eh increases of approximately 20 and 40 mV, respectively, in the EMB (Figure 7), which is a sufficient E_h change to alter patterns of proliferation and differentiation in the EMB. The specific redox-sensitive pathways, signaling nodes, and target proteins that may be responsible for preventing timely neural tube closure have not yet been identified.

Numerous temporal and spatial changes in the proportion of oxidized (GSSG, CySS) and reduced (GSH, Cys) species in the VYS and EMB occur across the 24 hr time course under *normal* culture conditions. Total GSH and CyS concentrations (reduced + 2X oxidized thiol), as well as the relative proportion of oxidized and reduced species they represent, fluctuate naturally in controls and may not be directly correlated with any specific growth or differentiation event. The addition of MEHP produces a generally consistent, but fluctuating, pattern of total GSH and CyS reduction without eliciting a significant net proportional shift towards greater oxidation (as indicated by E_h). The initial spike in total GSH and total CyS observed at 1 h is very transient and is believed to result as an adaptation from the initial shock of explant and introduction into culture, athough, this effect was modified by MEHP. These increases and their subsequent return to the normal range are not accompanied by a net shift in E_h (Figure 7). Across the 24 h time course, the E_h values remain relatively stable in the VYS until the tissues become highly reduced at 24 h. This pattern also holds for the EMB with the exception of the 12 h time point where a significant dose-dependent oxidation occurs. Again, this time-specific oxidation at 12 h coincides with several critical physiological, differentiation, and growth-sensitive developmental transitions such as neural tube closure, which might be related mechanistically. The control mouse VYS and EMB also appear to be much more oxidized at the onset of culture on GD8 compared to the rat (GD10) at a comparable stage of development. This trend continues through 12 h of culture in the mouse. This may indicate that the enzymes responsible for GSH biosynthesis and regulation are late to mature in the mouse, as has been shown for other metabolic and biotransformation enzyme activities [71]. Optimal reducing environments, in which GSH E_h values drop below −230 mV, are reached and sustained by 24 h in mWEC (GD 9).

The meaningful identification and comparison of disparate measures such as growth, morphogenesis, and redox status would be greatly enhanced with the identification and characterization of precise quantitative endpoints for embryotoxicity. In order to narrow the search to relevant targets and pathways we have attempted to superimpose an analysis of gene expression over the growth, anatomical, and biochemical parameters. Because a complete temporal ontogeny profile was not possible for the current analysis we chose to evaluate only the spatial VYS and EMB expressions at the 6 h time point. The rationale for assessment of expression at 6 h was based on a perceived need to avoid the period of culture adjustments (1 h – 3 h) but still to preceed the major genetic and physiological events that accompany the onset of active heartbeat and related metabolic events around the 12 h point.

The 6 h time point sepresents a cumulative expression profile representative of all normal and MEHP-induced events elicited over the first 6 h of culture. One major consideration that is often overlooked in the evaluation of expression data in complex tissues such as are seen in the developing conceptus is the contribution of multiple cell types to the overall expression profile. This is particularly important in the conceptus where many different types of cells are constantly emerging as the three primary germ layers differentiate, migrate, expand, and die as they follow the developmental program. The VYS is most often discarded as irrelevant in developmental assessments although its active circulation, metabolic contributions, and nutritive functions are intimately associated and completely essential to EMB growth and development. Comparative gene expression data (Table 2) shows five MEHP-disrupted pathways that were identified from the KEGG database and which are common to both EMB and VYS. These can be collectively identified as pathways related to *oxidative phosphorylation* and *amino acid metabolism*. It is not surprising, perhaps, that the EMB also has altered expression in pathways associated with nutrient metabolism, protein recycling and membrane transport, while the VYS displays alterations in pathways required for xenobiotic biotransformation such as *glutathione metabolism*, *drug metabolism-cytochrome P450*, and *selenocompound metabolism*. The VYS also shows significant changes in pathways related to *ribosome biogenesis* and *aminoacyl-tRNA biosynthesis*, which have been noted in other studies as being consequences of amino acid starvation and the likely activation or misregulation of autophagy [36, 72, 73]. The perturbation of expression related to the latter pathways are in accord with other studies using a variety of xenobiotics and chemical modulators which suggest that the disruption of conceptal nutrient uptake may be a contributory factor in these outcomes [36, 72, 73]. This concept agrees with previous studies showing that inhibition of the histiotrophic nutrition pathways (HNP), through which the vast majority of conceptal nutrients are obtained, results in convincing proteomic evidence that the activation of *ribosome biogenesis* and *autophagy* pathways are selective indicators of toxicity. We have previously demonstrated that MEHP significantly reduces HNP activity in the mouse model used in the study [74]. This indicates that MEHP-induced changes in nutrient availability and processing could be a factor in observed developmental toxicity.

In this study, mRNA expression related to numerous pathways involved in amino acid metabolism were disrupted, such as the metabolism of alanine, aspartate, glutamate, arginine, proline, and histidine. Additional indirect amino acid metabolic pathways, such as GSH metabolism and TCA cycle were also affected. Because all of these pathways rely on the supply of amino acids, it is possible that MEHP treatment is inducing a form of amino acid starvation through decreased nutrient availability as previously found [74]. Amino acid starvation has been discovered to have numerous physiological and metabolic consequences, namely effects on energy metabolism including oxidative phosphorylation [75, 76]. MEHP has been demonstrated to decrease protein uptake into the conceptus, reducing the amino acids available for protein synthesis and metabolism [74]. It is therefore likely that MEHP-induced amino acid starvation could have numerous downstream consequences affecting signaling and overall growth and differentiation. The decreased size of embryos exposed to MEHP raises questions regarding the implications of phthalates on both growth and also potential metabolic diseases later in life. Furthermore, *vitamin transport* was downregulated

in both the EMB and VYS, supporting the concept that a nutritional deficiency could be occurring. Transport of folate, one of the primary nutrients protective against NTDs, was downregulated, and provides a potential mechanism for investigation for MEHP-related NTDs.

Oxidative phosphorylation was the most significantly affected pathway for both EMB and VYS due to phthalate treatment based on the bioinformatics analysis, but was upregulated in the VYS and downregulated in the EMB. The changes in oxidative phosphorylation processes observed are indicative of MEHP-induced dysregulation of energy metabolism processes. Increases in the expression of ATPases, some of the most redox-sensitive proteins in the cell, suggest the necessity to maintain cellular homeostasis and potential mitochondrial ion gradients during toxicant-induced physiological changes in the cell [77–82]. Likewise, decreases in the expression of ATP synthases in the EMB could be indicative of decreased substrates available for energy production (ATP-form) in the cell. This suggests that the ability to produce ATP is compromised, and yet the energy demands are growing.

The brain has very high energy demands, and relies heavily on oxidative phosphorylation and mitochondrial function [83]. It is not surprising that this time in development would be very susceptible to changes in oxidative phosphorylation, since large increases in mitochondrial density and mitochondrial proteins are initiated at the beginning of neurogenesis [84]. Changes to the oxidative phosphorylation pathway have been previously demonstrated to be altered by exposures in the brain and NTDs [85, 86]. Because oxidative phosphorylation requires the coordination of numerous enzymes and energy substrates, as well as maintenance of a high-energy proton gradient, these processes are often decreased in starved cells. These cells then rely on the more efficient but lower energy payout process of glycolysis. During this phase of organogenesis, oxidative phosphorylation processes are only initiating, and the embryo mostly relies on glycolysis for ATP generation. However, inhibition of oxidative phosphorylation during this window frequently results in NTDs and embryolethality in mouse models [54–56]. In this study, the GO Biological Process *oxidative phosphorylation* was decreased in the EMB, though further mechanistic work is necessary to determine whether this decrease contributes to the NTD phenotypes observed in this study.

Disruption of oxidative phosphorylation and amino acid metabolism, oxidation of GSH/GSSG redox potential, decreased vitamin transport processes, compounded with prior evidence of decreased nutritional clearance, suggest that MEHP treatment can produce severe nutritional deficiencies during early organogenesis [74]. Often during such deficiencies, processes governing mitochondrial function are stimulated or supported at the expense of cytosolic processes [87]. Expression changes to enzymes involved with amino acid metabolism, GSH metabolism, TCA cycle, and oxidative phosphorylation, coupled to the expression changes observed in the SLC25 mitochondrial transporters class suggest that this shunting and prioritization of the maintenance of mitochondrial functions is beginning to occur at this 6 h time point. Metabolic biological processes significantly changed by MEHP exposure were regulated differently in the EMB and VYS, often with increased metabolic capacity in the VYS and decreased activity in the EMB. It is likely that the VYS is preserving its function as a metabolic barrier for the EMB, but this is occurring at the

energetic expense of the EMB. Further mechanistic work to study the metabolic consequences of MEHP exposure on EMB and VYS mitochondrial function, is necessary to characterize the specific energetic effects in the EMB and VYS.

Although the KEGG data shown in Table 2 gives a good picture of the major expression changes induced by MEHP in VYS and EMB, they do not show many important additional details about the direction of expression changes which are instructive for optimal interpretation. In order to extend this analysis, we have plotted expression data sorted by gene ontology (GO) coding. Altered gene expression patterns in MEHP-exposed conceptal tissues are shown in Figure 8 as a distribution of *GO Biological Processes*. The GO terms represent molecular events or other beginning-to-end operations that are integrated across the spectrum of biological organization from cells to the whole organism. Expression changes for EMB are distributed along the Y-axis where positive values represent increased expression and negative values decreased expression. The X-axis shows distribution in the VYS from positive to negative in like fashion. General patterns of distribution show that the prominent effect of MEHP exposure in the whole conceptus is to increase gene expression in the EMB and decrease expression in the VYS. GO terms differentially clustered in this manner are those associated with *amino acid metabolism*, *metabolic processes*, *cellular processes*, and localization, indicating that the EMB is mounting a positive adaptive response to the chemical insult. Concurrent down-regulation of the same processes in the VYS suggests that it is undergoing a more conservative adaptive response. GO terms most prominent in the quadrant where gene expression is increased in both EMB and VYS are those for *developmental processes*, *biological regulation*, *negative regulation of peptidyl-serine phosphorylation*, and a cluster related to *kidney development*. An even smaller number of GO terms mapped to the quadrant for increased VYS expression and decreased EMB expression where clusters for *oxidative phosphorylation & etc*. and *iron-sulfur cluster assembly* along with *response to stimulus*, *metabolic processes* and *localization* predominate. The only GO term that was found to be associated with decreased expression in both EMB and VYS mapped to *vitamin transport*. This analysis suggests that the two major common alterations in MEHP-induced gene expression: *oxidative phosphorylation* and *amino acid metabolism/activation* (Table 2) identified by KEGG pathways, represent increased VYS expression/decreased EMB expression and increased EMB expression/decreased VYS expression, respectively. Decreased oxidative phosphorylation and increased amino acid metabolism are conditions generally associated with the activation of autophagy, otherwise known as ‘programmed cell survival’. This pattern agrees with proteomic results from previous studies where rat conceptuses were exposed to GSH modulators, protease inhibitors, and embryotoxins where changes in protein concentrations mapped to similar pathways [36, 72, 73].

Results from this spatial and temporal evaluation of EMB and VYS morphology, redox status, and gene expression during early mouse organogenesis, highlights several of the inherent difficulties in identifying specific mechanistic associations between changes in redox status and adverse structural and functional outcomes. The phthalate, MEHP, elicits significant increases in E_h in both EMB and VYS which are based on the altered relative concentrations of oxidized and reduced thiol species for the GSSG/GSH and CySS/CyS redox couples. Neither thiol concentrations nor their respective E_h values remain constant

during mouse organogenesis, but rather, fluctuate spatially and temporally in EMB and VYS. The lack of concordance between the two tissues and over time suggest that, even though EMB and VYS are intimately connected and share a common circulatory system, they are regulated independently. The observed differential patterns of gene expression support this conclusion and suggest possible MEHP targets to examine for their roles in eliciting embryotoxicity and causing neural tube defects. Gene expression pathways related to *oxidative phosphorylation* were significantly upregulated in the VYS and downregulated in the EMB, while pathways for *amino acid metabolism* were significantly upregulated in the EMB and downregulated in the VYS, suggesting attempts to differentially increase energy production or metabolism in one tissue and to conserve activity in another. The roles of these changes, along with decreases in processes such as *vitamin transport*, other *solute carrier transporters*, *developmental processes*, and *metabolic processes*, have yet to be linked specifically and mechanistically with redox states or the specific etiology of neural tube defects. Based on the results presented here, it is not clear whether MEHP induces changes in E_h that lead to altered differential gene expression and improper neural tube closure or whether MEHP first alters gene expression that then leads to alterations in E_h and the formation of neural tube defects.

Supplementary Material

Refer to Web version on PubMed Central for supplementary material.

Acknowledgments

We would like to acknowledge Grace Kuan, Lindsey Jacobs, and Erin Scarlett for their laboratory support. This work was supported by the Bill and Melinda Gates Foundation (Grand Challenges Explorations – Rd. 7) and the University of Michigan National Institute of Environmental Health Sciences (NIEHS) Core Center “Lifestage Environmental Exposures and Disease” (M-LEEaD; P30 ES017885). Support was also provided to K.E.S. by an NRSA institutional training grant (T32 ES007062).

References

1. Cai J, Cheng A, Luo Y, Lu C, Mattson MP, Rao MS, et al. Membrane properties of rat embryonic multipotent neural stem cells. J Neurochem. 2004; 88:212–26. [PubMed: 14675165]
2. Cove DJ. The generation and modification of cell polarity. Journal of Experimental Botany. 2000; 51:831–8. [PubMed: 10948208]
3. Thiery JP, Duband JL, Tucker GC. Cell Migration in the Vertebrate Embryo: Role of Cell Adhesion and Tissue Environment in Pattern Formation. Annual Review of Cell Biology. 1985; 1:91–113.
4. Tsujioka M. Cell migration in multicellular environments. Development, growth & differentiation. 2011; 53:528–37.
5. Hansen JM, Harris C. Redox control of teratogenesis. Reproductive Toxicology. 2013; 35:165–79. [PubMed: 23089153]
6. Jones DP. Redefining oxidative stress. Antioxidants & redox signaling. 2006; 8:1865–79. [PubMed: 16987039]
7. Ornoy A. Prenatal origin of obesity and their complications: Gestational diabetes, maternal overweight and the paradoxical effects of fetal growth restriction and macrosomia. Reproductive Toxicology. 2011; 32:205–12. [PubMed: 21620955]
8. Wan J, Winn LM. In utero–initiated cancer: The role of reactive oxygen species. Birth Defects Research Part C: Embryo Today: Reviews. 2006; 78:326–32.

9. Jeng W, Wong AW, Ting-A-Kee R, Wells PG. Methamphetamine-enhanced embryonic oxidative DNA damage and neurodevelopmental deficits. Free Radical Biology and Medicine. 2005; 39:317–26. [PubMed: 15993330]
10. Zhou, L.; Beattie, MC.; Lin, C-Y.; Liu, J.; Traore, K.; Papadopoulos, V., et al. Reproductive toxicology. Elmsford, NY: 2013. Oxidative Stress and Phthalate-Induced Down-Regulation of Steroidogenesis in MA-10 Leydig Cells*. 0:10.1016/j.reprotox.2013.07.025
11. Rusyn I, Kadiiska MB, Dikalova A, Kono H, Yin M, Tsuchiya K, et al. Phthalates rapidly increase production of reactive oxygen species in vivo: role of Kupffer cells. Molecular pharmacology. 2001; 59:744–50. [PubMed: 11259618]
12. Erkekoğlu P, Rachidi W, Yüzügüllü OG, Giray B, Öztürk M, Favier A, et al. Induction of ROS, p53, p21 in DEHP- and MEHP-exposed LNCaP cells-protection by selenium compounds. Food and Chemical Toxicology. 2011; 49:1565–71. [PubMed: 21515331]
13. Tetz LM, Cheng AA, Korte CS, Giese RW, Wang P, Harris C, et al. Mono-2-ethylhexyl phthalate induces oxidative stress responses in human placental cells in vitro. Toxicology and Applied Pharmacology. 2013; 268:47–54. [PubMed: 23360888]
14. Ray PD, Huang B-W, Tsuji Y. Reactive oxygen species (ROS) homeostasis and redox regulation in cellular signaling. Cellular signalling. 2012; 24:981–90. [PubMed: 22286106]
15. D'Autreaux B, Toledano MB. ROS as signalling molecules: mechanisms that generate specificity in ROS homeostasis. Nat Rev Mol Cell Biol. 2007; 8:813–24. [PubMed: 17848967]
16. Finkel T. Signal transduction by reactive oxygen species. The Journal of cell biology. 2011; 194:7–15. [PubMed: 21746850]
17. Schafer FQ, Buettner GR. Redox environment of the cell as viewed through the redox state of the glutathione disulfide/glutathione couple. Free Radical Biology and Medicine. 2001; 30:1191–212. [PubMed: 11368918]
18. Harris, C.; Hansen, J.; Oxidative, Stress. Thiols, and Redox Profiles. In: Harris, C.; Hansen, JM., editors. Developmental Toxicology. Humana Press; 2012. p. 325-46.
19. Surh YJ, Kundu JK, Na HK. Nrf2 as a master redox switch in turning on the cellular signaling involved in the induction of cytoprotective genes by some chemopreventive phytochemicals. Planta medica. 2008; 74:1526–39. [PubMed: 18937164]
20. Erkekoglu P, Rachidi W, Yuzugullu OG, Giray B, Favier A, Ozturk M, et al. Evaluation of cytotoxicity and oxidative DNA damaging effects of di(2-ethylhexyl)-phthalate (DEHP) and mono(2-ethylhexyl)-phthalate (MEHP) on MA-10 Leydig cells and protection by selenium. Toxicology and Applied Pharmacology. 2010; 248:52–62. [PubMed: 20659492]
21. Lin S, Ku H-Y, Su P-H, Chen J-W, Huang P-C, Angerer J, et al. Phthalate exposure in pregnant women and their children in central Taiwan. Chemosphere. 2011; 82:947–55. [PubMed: 21075419]
22. Lin L. Levels of environmental endocrine disruptors in umbilical cord blood and maternal blood of low-birth-weight infants. Zhōnghuá yùfáng-yīxué zázhì. 2008; 42:177–80. [PubMed: 18788582]
23. Huang P-C, Kuo P-L, Chou Y-Y, Lin S-J, Lee C-C. Association between prenatal exposure to phthalates and the health of newborns. Environment International. 2009; 35:14–20. [PubMed: 18640725]
24. Mose T, Mortensen GK, Hedegaard M, Knudsen LE. Phthalate monoesters in perfusate from a dual placenta perfusion system, the placenta tissue and umbilical cord blood. Reproductive Toxicology. 2007; 23:83–91. [PubMed: 17049806]
25. Stroheker T, Regnier J-F, Lassurguere J, Chagnon M-C. Effect of in utero exposure to di-(2-ethylhexyl)phthalate: Distribution in the rat fetus and testosterone production by rat fetal testis in culture. Food and Chemical Toxicology. 2006; 44:2064–9. [PubMed: 16979278]
26. Calafat AM, Brock JW, Silva MJ, Gray LE Jr, Reidy JA, Barr DB, et al. Urinary and amniotic fluid levels of phthalate monoesters in rats after the oral administration of di(2-ethylhexyl) phthalate and di-n-butyl phthalate. Toxicology. 2006; 217:22–30. [PubMed: 16171919]
27. Latini G, Felice Cd, Presta G, Vecchio Ad, Paris I, Ruggieri F, et al. In Utero Exposure to Di-(2-Ethylhexyl)phthalate and Duration of Human Pregnancy. Environmental health perspectives. 2003; 111:1783–5. [PubMed: 14594632]

28. Latini G, De Felice C, Presta G, Del Vecchio A, Paris I, Ruggieri F, et al. Exposure to Di(2-ethylhexyl)phthalate in Humans during Pregnancy. Neonatology. 2003; 83:22–4.
29. Chu D-P, Tian S, Qi L, Hao C-J, Xia H-F, Ma X. Abnormality of maternal-to-embryonic transition contributes to MEHP-induced mouse 2-cell block. Journal of Cellular Physiology. 2013; 228:753–63. [PubMed: 22949295]
30. Onorato TM, Brown PW, Morris PL. Mono-(2-ethylhexyl) Phthalate Increases Spermatocyte Mitochondrial Peroxiredoxin 3 and Cyclooxygenase 2. Journal of Andrology. 2008; 29:293–303. [PubMed: 18077825]
31. Hansen JM, Gong S-G, Philbert M, Harris C. Misregulation of gene expression in the redox-sensitive NF-κb-dependent limb outgrowth pathway by thalidomide. Developmental Dynamics. 2002; 225:186–94. [PubMed: 12242718]
32. Hansen JM, Carney EW, Harris C. Altered differentiation in rat and rabbit limb bud micromass cultures by glutathione modulating agents. Free Radical Biology and Medicine. 2001; 31:1582–92. [PubMed: 11744332]
33. McNutt TL, Harris C. Lindane embryotoxicity and differential alteration of cysteine and glutathione levels in rat embryos and visceral yolk sacs. Reproductive Toxicology. 1994; 8:351–62. [PubMed: 7524828]
34. Hiranruengchok R, Harris C. Glutathione Oxidation and Embryotoxicity Elicited by Diamide in the Developing Rat Conceptus in Vitro. Toxicology and Applied Pharmacology. 1993; 120:62–71. [PubMed: 8511783]
35. Sahambi SK, Hales BF. Exposure to 5-Bromo-2′-deoxyuridine induces oxidative stress and activator protein-1 DNA binding activity in the embryo. Birth Defects Research Part A: Clinical and Molecular Teratology. 2006; 76:580–91.
36. Harris C, Shuster DZ, Roman Gomez R, Sant KE, Reed MS, Pohl J, et al. Inhibition of glutathione biosynthesis alters compartmental redox status and the thiol proteome in organogenesis-stage rat conceptuses. Free Radical Biology and Medicine. 2013; 63:325–37. [PubMed: 23736079]
37. Thompson SA, White CC, Krejsa CM, Eaton DL, Kavanagh TJ. Modulation of Glutathione and Glutamate-L-cysteine Ligase by Methylmercury during Mouse Development. Toxicological Sciences. 2000; 57:141–6. [PubMed: 10966520]
38. Jilek JL, Sant KE, Cho KH, Reed MS, Pohl J, Hansen JM, et al. Ethanol Attenuates Histiotrophic Nutrition Pathways and Alters the Intracellular Redox Environment and Thiol Proteome during Rat Organogenesis. Toxicological Sciences. 2015
39. Harris, C. Rodent Whole Embryo Culture. In: Harris, C.; Hansen, JM., editors. Developmental Toxicology. Humana Press; 2012. p. 215-37.
40. Janer G, Verhoef A, Gilsing HD, Piersma AH. Use of the rat postimplantation embryo culture to assess the embryotoxic potency within a chemical category and to identify toxic metabolites. Toxicology in Vitro. 2008; 22:1797–805. [PubMed: 18675337]
41. Robinson JF, Verhoef A, van Beelen VA, Pennings JLA, Piersma AH. Dose–response analysis of phthalate effects on gene expression in rat whole embryo culture. Toxicology and Applied Pharmacology. 2012; 264:32–41. [PubMed: 22841773]
42. Stoscheck C. Quantification of Protein. Methods in Enzymology. 1990; 182:50–69. [PubMed: 2314256]
43. Jones DP, Carlson JL, Samiec PS, Sternberg P Jr, Mody VC Jr, Reed RL, et al. Glutathione measurement in human plasma: Evaluation of sample collection, storage and derivatization conditions for analysis of dansyl derivatives by HPLC. Clinica Chimica Acta. 1998; 275:175–84.
44. Smyth GK. Linear models and empirical bayes methods for assessing differential expression in microarray experiments. Statistical applications in genetics and molecular biology. 2004; 3 Article3.
45. Sartor MA, Leikauf GD, Medvedovic M. LRpath: a logistic regression approach for identifying enriched biological groups in gene expression data. Bioinformatics. 2009; 25:211–7. [PubMed: 19038984]
46. Banerjee R. Redox outside the Box: Linking Extracellular Redox Remodeling with Intracellular Redox Metabolism. Journal of biological chemistry. 2012; 287:4397–402. [PubMed: 22147695]

47. Hansen JM, Harris C. Glutathione during embryonic development. Biochimica et Biophysica Acta (BBA) - General Subjects. 2015; 1850:1527–42. [PubMed: 25526700]
48. Hoglund PJ, Nordstrom KJ, Schioth HB, Fredriksson R. The solute carrier families have a remarkably long evolutionary history with the majority of the human families present before divergence of Bilaterian species. Molecular biology and evolution. 2011; 28:1531–41. [PubMed: 21186191]
49. Institute of Biochemistry and Molecular Medicine. SLC Tables. Bioparadigmsorg. Bern: Switzerland University of Bern; 2004.
50. Palmieri F. The mitochondrial transporter family SLC25: Identification, properties and physiopathology. Molecular Aspects of Medicine. 2013; 34:465–84. [PubMed: 23266187]
51. National Center for Biotechnology Information. SLC7A9. Gene Database. 2014
52. Jauniaux E, Watson AL, Hempstock J, Bao YP, Skepper JN, Burton GJ. Onset of maternal arterial blood flow and placental oxidative stress. A possible factor in human early pregnancy failure. The American journal of pathology. 2000; 157:2111–22. [PubMed: 11106583]
53. Jauniaux E, Watson A, Burton G. Evaluation of respiratory gases and acid-base gradients in human fetal fluids and uteroplacental tissue between 7 and 16 weeks' gestation. American Journal of Obstetrics and Gynecology. 2001; 184:998–1003. [PubMed: 11303211]
54. Li K, Li Y, Shelton JM, Richardson JA, Spencer E, Chen ZJ, et al. Cytochrome c Deficiency Causes Embryonic Lethality and Attenuates Stress-Induced Apoptosis. Cell. 2000; 101:389–99. [PubMed: 10830166]
55. Nonn L, Williams RR, Erickson RP, Powis G. The Absence of Mitochondrial Thioredoxin 2 Causes Massive Apoptosis, Exencephaly, and Early Embryonic Lethality in Homozygous Mice. Molecular and cellular biology. 2003; 23:916–22. [PubMed: 12529397]
56. Piruat JI, Pintado CO, Ortega-Sáenz P, Roche M, López-Barneo J. The Mitochondrial SDHD Gene Is Required for Early Embryogenesis, and Its Partial Deficiency Results in Persistent Carotid Body Glomus Cell Activation with Full Responsiveness to Hypoxia. Molecular and cellular biology. 2004; 24:10933–40. [PubMed: 15572694]
57. Robinson JF, van Beelen VA, Verhoef A, Renkens MFJ, Luijten M, van Herwijnen MHM, et al. Embryotoxicant-Specific Transcriptomic Responses in Rat Postimplantation Whole-Embryo Culture. Toxicological Sciences. 2010; 118:675–85. [PubMed: 20864626]
58. Fairbairn EA, Bonthius J, Cherr GN. Polycyclic aromatic hydrocarbons and dibutyl phthalate disrupt dorsal–ventral axis determination via the Wnt/β-catenin signaling pathway in zebrafish embryos. Aquatic Toxicology. 2012:124–125. 188–96. [PubMed: 23291050]
59. Webster WS, Brown-Woodman PD, Ritchie HE. A review of the contribution of whole embryo culture to the determination of hazard and risk in teratogenicity testing. The International journal of developmental biology. 1997; 41:329–35. [PubMed: 9184342]
60. Wang W, Craig ZR, Basavarajappa MS, Hafner KS, Flaws JA. Mono-(2-ethylhexyl) phthalate induces oxidative stress and inhibits growth of mouse ovarian antral follicles. Biol Reprod. 2012; 87:152. [PubMed: 23077170]
61. Hansen JM. Oxidative stress as a mechanism of teratogenesis. Birth defects research Part C, Embryo today: reviews. 2006; 78:293–307.
62. Chu D-P, Tian S, Sun D-G, Hao C-J, Xia H-F, Ma X. Exposure to mono-n-butyl phthalate disrupts the development of preimplantation embryos. Reproduction, Fertility and Development. 2013; 25:1174–84.
63. Xu H, Shao X, Zhang Z, Zou Y, Wu X, Yang L. Oxidative stress and immune related gene expression following exposure to di-n-butyl phthalate and diethyl phthalate in zebrafish embryos. Ecotoxicology and environmental safety. 2013; 93:39–44. [PubMed: 23676468]
64. Aw TY. Cellular Redox: A Modulator of Intestinal Epithelial Cell Proliferation. 2003
65. Droge W. Free radicals in the physiological control of cell function. Physiological reviews. 2002; 82:47–95. [PubMed: 11773609]
66. Shi X, Zhang Y, Zheng J, Pan J. Reactive oxygen species in cancer stem cells. Antioxidants & redox signaling. 2012; 16:1215–28. [PubMed: 22316005]
67. Pervaiz S, Taneja R, Ghaffari S. Oxidative stress regulation of stem and progenitor cells. Antioxidants & redox signaling. 2009; 11:2777–89. [PubMed: 19650689]

68. Acharya A, Das I, Chandhok D, Saha T. Redox regulation in cancer: a double-edged sword with therapeutic potential. Oxidative medicine and cellular longevity. 2010; 3:23–34. [PubMed: 20716925]
69. Kovacic P, Somanathan R. Mechanism of teratogenesis: electron transfer, reactive oxygen species, and antioxidants. Birth defects research Part C, Embryo today: reviews. 2006; 78:308–25.
70. Harris C, Hansen JM. Oxidative stress, thiols, and redox profiles. Methods Mol Biol. 2012; 889:325–46. [PubMed: 22669675]
71. Harris C, Wang S-W, Lauchu JJ, Hansen JM. Methanol metabolism and embryotoxicity in rat and mouse conceptuses: comparisons of alcohol dehydrogenase (ADH1), formaldehyde dehydrogenase (ADH3), and catalase. Reproductive Toxicology. 2003; 17:349–57. [PubMed: 12759105]
72. Harris C, Jilek JL, Sant KE, Pohl J, Reed M, Hansen JM. Amino acid starvation induced by protease inhibition produces differential alterations in redox status and the thiol proteome in organogenesis-stage rat embryos and visceral yolk sacs. Journal of nutritional biochemistry. 2015; 26:1589–98. [PubMed: 26365578]
73. Jilek JL, Sant KE, Cho KH, Reed MS, Pohl J, Hansen JM, et al. Ethanol Attenuates Histiotrophic Nutrition Pathways and Alters the Intracellular Redox Environment and Thiol Proteome during Rat Organogenesis. Toxicological Sciences. 2015; 147:475–89. [PubMed: 26185205]
74. Sant KE, Dolinoy DC, Jilek JL, Shay BJ, Harris C. Mono-2-ethylhexyl phthalate (MEHP) alters histiotrophic nutrition pathways and epigenetic processes in the developing conceptus. Journal of nutritional biochemistry. 2016; 27:211–8. [PubMed: 26507544]
75. Johnson MA, Vidoni S, Durigon R, Pearce SF, Rorbach J, He J, et al. Amino Acid Starvation Has Opposite Effects on Mitochondrial and Cytosolic Protein Synthesis. PLoS ONE. 2014; 9:e93597. [PubMed: 24718614]
76. Harris C, Jilek JL, Sant KE, Pohl J, Reed MS, Hansen JM. Amino Acid Starvation Induced by Protease Inhibition Produces Differential Alterations in Redox Status and the Thiol Proteome in Organogenesis-Stage Rat Embryos and Visceral Yolk Sacs. Journal of nutritional biochemistry. 2015
77. Petrushanko IY, Yakushev S, Mitkevich VA, Kamanina YV, Ziganshin RH, Meng X, et al. S-glutathionylation of the Na,K-ATPase catalytic alpha subunit is a determinant of the enzyme redox sensitivity. J Biol Chem. 2012; 287:32195–205. [PubMed: 22798075]
78. Liu J, Kennedy DJ, Yan Y, Shapiro JI. Reactive Oxygen Species Modulation of Na/K-ATPase Regulates Fibrosis and Renal Proximal Tubular Sodium Handling. Int J Nephrol. 2012; 2012:381320. [PubMed: 22518311]
79. Petrushanko I, Bogdanov N, Bulygina E, Grenacher B, Leinsoo T, Boldyrev A, et al. Na-K-ATPase in rat cerebellar granule cells is redox sensitive. American journal of physiology Regulatory, integrative and comparative physiology. 2006; 290:R916–25.
80. Comellas AP, Dada LA, Lecuona E, Pesce LM, Chandel NS, Quesada N, et al. Hypoxia-Mediated Degradation of Na,K-ATPase via Mitochondrial Reactive Oxygen Species and the Ubiquitin-Conjugating System. Circulation Research. 2006; 98:1314–22. [PubMed: 16614303]
81. Liu J, Tian J, Haas M, Shapiro JI, Askari A, Xie Z. Ouabain interaction with cardiac Na+/K+-ATPase initiates signal cascades independent of changes in intracellular Na+ and Ca2+ concentrations. J Biol Chem. 2000; 275:27838–44. [PubMed: 10874029]
82. Formentini L, Sanchez-Arago M, Sanchez-Cenizo L, Cuezva JM. The mitochondrial ATPase inhibitory factor 1 triggers a ROS-mediated retrograde prosurvival and proliferative response. Mol Cell. 2012; 45:731–42. [PubMed: 22342343]
83. Kann O, Kovacs R. Mitochondria and neuronal activity. American journal of physiology Cell physiology. 2007; 292:C641–57. [PubMed: 17092996]
84. Cordeau-Lossouarn L, Vayssiere JL, Larcher JC, Gros F, Croizat B. Mitochondrial maturation during neuronal differentiation in vivo and in vitro. Biology of the cell/under the auspices of the European Cell Biology Organization. 1991; 71:57–65. [PubMed: 1912948]
85. Hong Y, Piao F, Zhao Y, Li S, Wang Y, Liu P. Subchronic exposure to arsenic decreased Sdha expression in the brain of mice. Neurotoxicology. 2009; 30:538–43. [PubMed: 19422848]

86. Wlodarczyk BJ, Cabrera RM, Hill DS, Bozinov D, Zhu H, Finnell RH. Arsenic-induced gene expression changes in the neural tube of folate transport defective mouse embryos. Neurotoxicology. 2006; 27:547–57. [PubMed: 16620997]

87. Lin TC, Chen YR, Kensicki E, Li AY, Kong M, Li Y, et al. Autophagy: resetting glutamine-dependent metabolism and oxygen consumption. Autophagy. 2012; 8:1477–93. [PubMed: 22906967]

Highlights

1. MEHP caused a high incidence of neural tube defects in mouse embryos grown in whole embryo culture.
2. GSH and Cys concentrations fluctuated spatially and temporally in embryo and visceral yolk sac.
3. Redox potentials for GSSG/GSH and CYSS/Cys showed treatment induced oxidations at 1, 3 and 12 h.
4. MEHP changed gene expression in oxidative phosphorylation, and amino acid metabolism pathways.
5. It is difficult to correlate spatial and temporal redox changes and gene expression with defects.

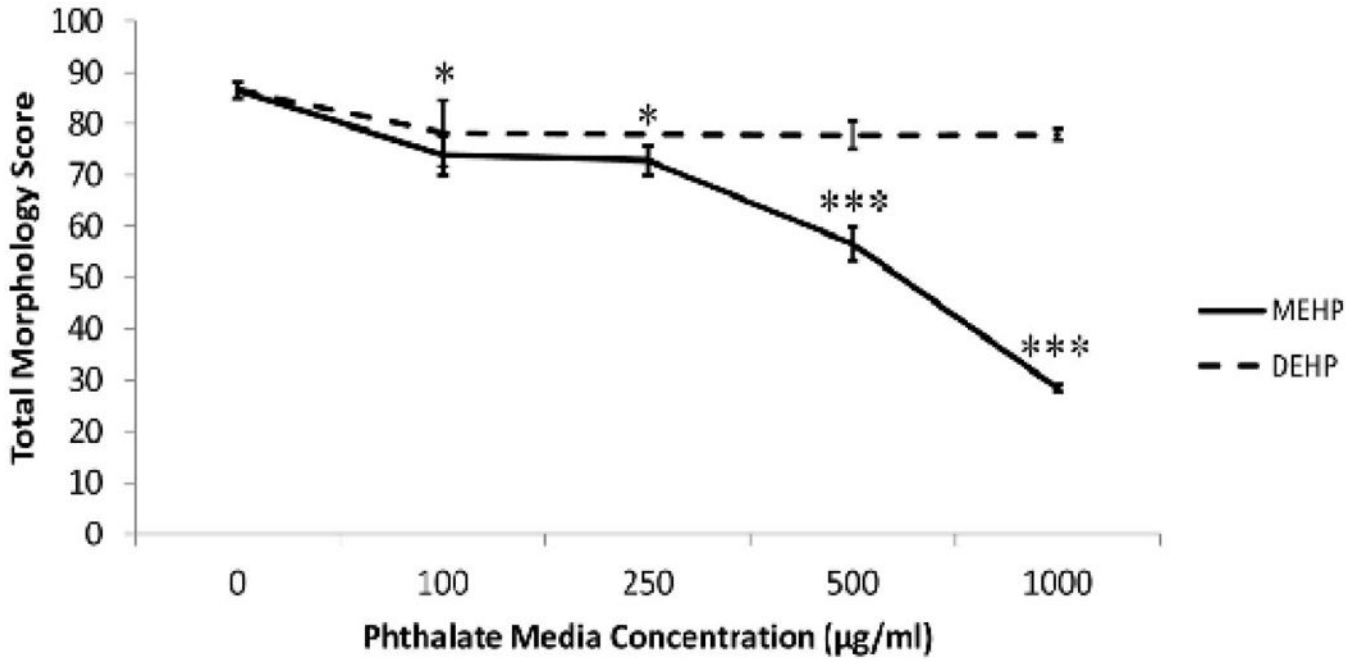

Figure 1.

MEHP treatment reduces overall morphological score. Unlike the parent compound DEHP, metabolite MEHP is able to reduce overall morphological scores in a dose-dependent manner after 24 h treatment in WEC. N=5 for all DEHP groups; sample sizes for MEHP groups are presented in Table 1. * indicates a significant change ($p<0.05$) in the MEHP group from the control at this dose. *** indicates a very significant change ($p<0.001$) in the MEHP group from the control at this dose. No significant changes were observed in DEHP-treated conceptuses.

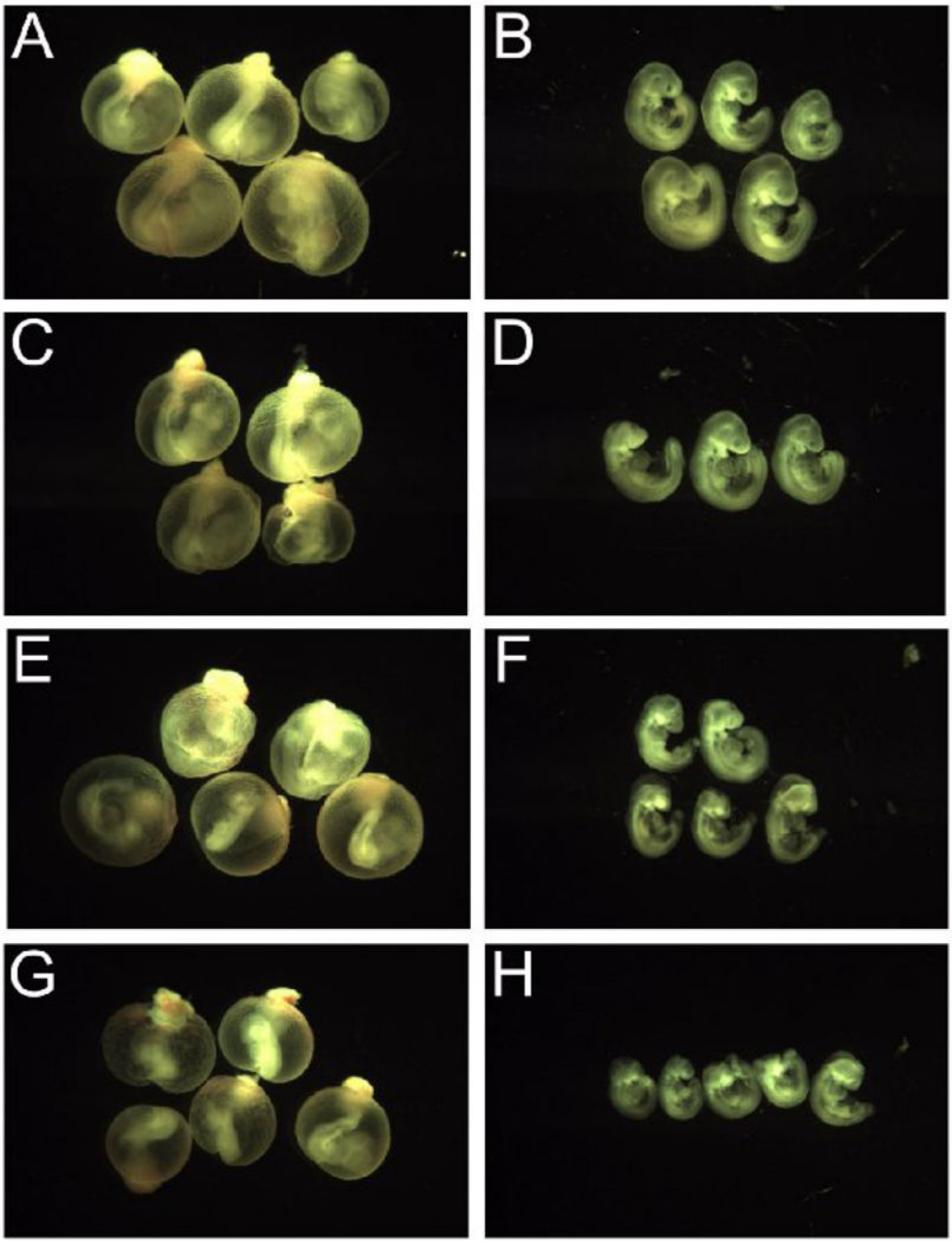

Figure 2.

MEHP decreases embryonic size and induces malformations. Images taken of the exposed conceptuses exposed to MEHP beginning on GD8 and cultured for 24 h reveal a gradual decrease in overall size and an increase in malformations as media MEHP concentrations increase. All images were taken at the same magnification. Image key: control (A&B), MEHP 100μg/ml (C&D), MEHP 500μg/ml (E&F), MEHP 1mg/ml (G&H).

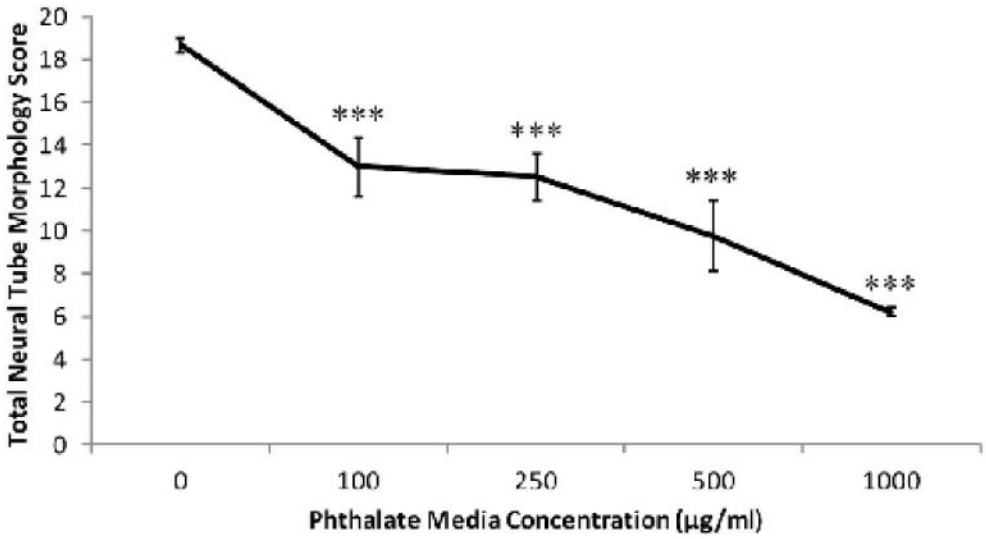

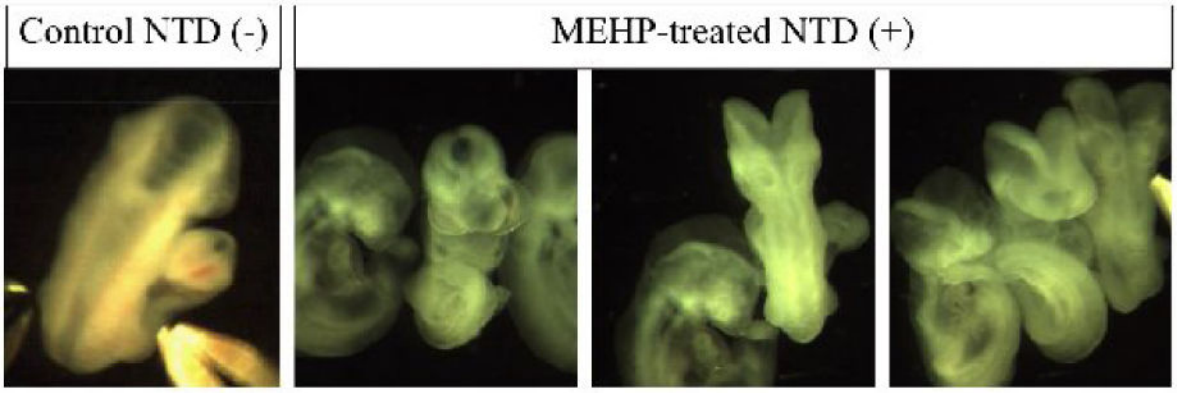

Figure 3.

MEHP treatment impairs neural tube closure in WEC. An unusually high number of open neural tubes were observed in the MEHP-treated groups after 24 h treatment. Some of those malformations are shown above. Overall, with increased concentration of MEHP in the culture media, there is a reduction of neural tube scores. The highest possible total neural tube score attainable is 20, and scores are reduced by characteristics such as an open neural tube, necrotic debris present in the neural tube, and hypoplastic tissues around the brain regions. *** indicates a very significant change ($p<0.001$) in the MEHP group from the control at this dose.

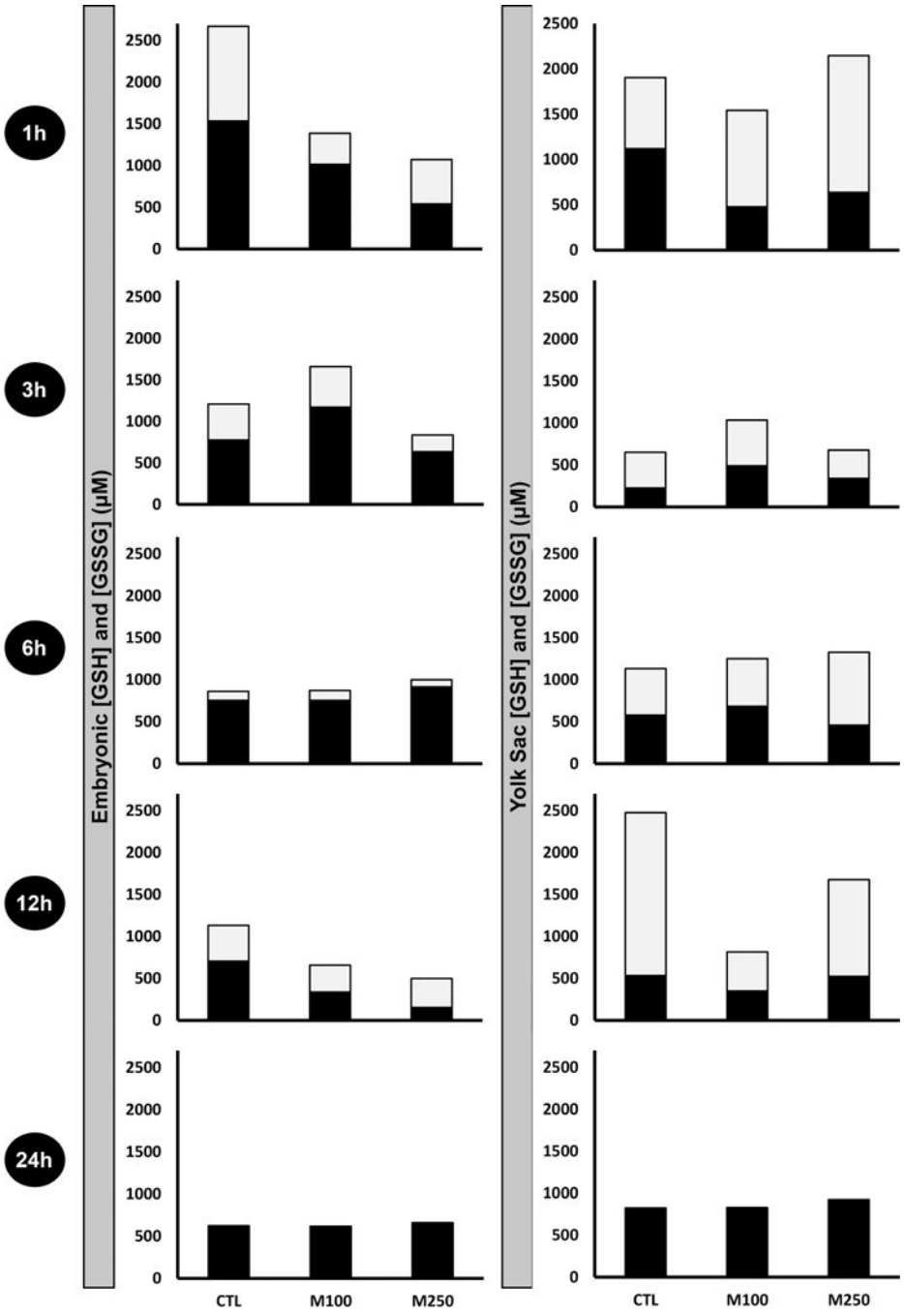

Figure 4.

Ontogeny of reduced and oxidized glutathione measurements in EMB and VYS following MEHP treatment. Black fractions represent the concentrations (μM) of reduced glutathione (GSH), and gray fractions represent the concentrations (μM) of oxidized glutathione (GSSG). Results from each analysis group represent a total of 4–8 EMB or VYS samples, collected from individual conceptuses and randomized from multiple litters.

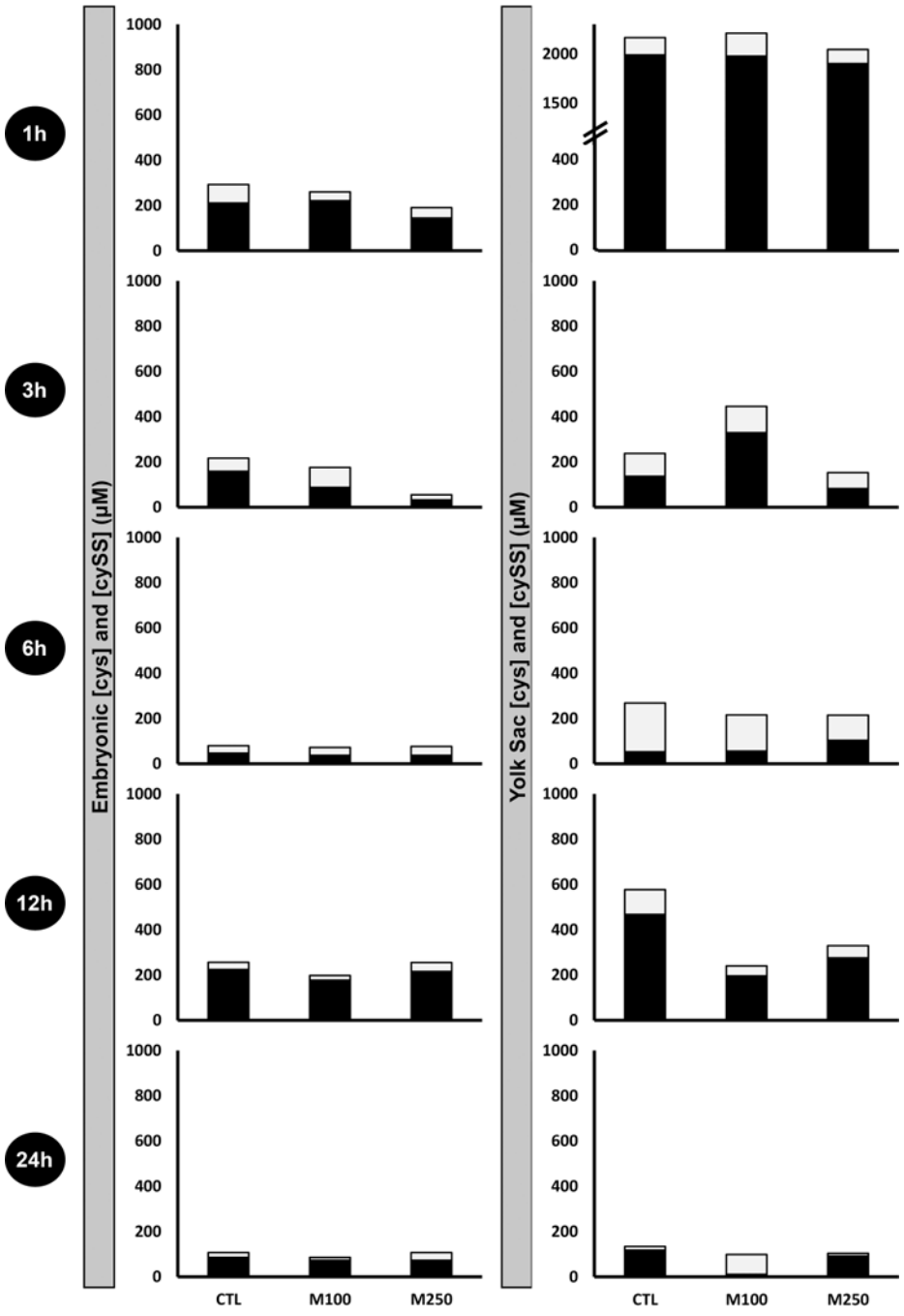

Figure 5.

Ontogeny of reduced and oxidized cysteine measurements in EMB and VYS following MEHP treatment. Black fractions represent the concentrations (μM) of reduced cysteine (Cys), and gray fractions represent the concentrations (μM) of oxidized cystine (CySS). Results from each analysis group represent a total of 4–8 EMB or VYS samples, collected from individual conceptuses and randomized from multiple litters.

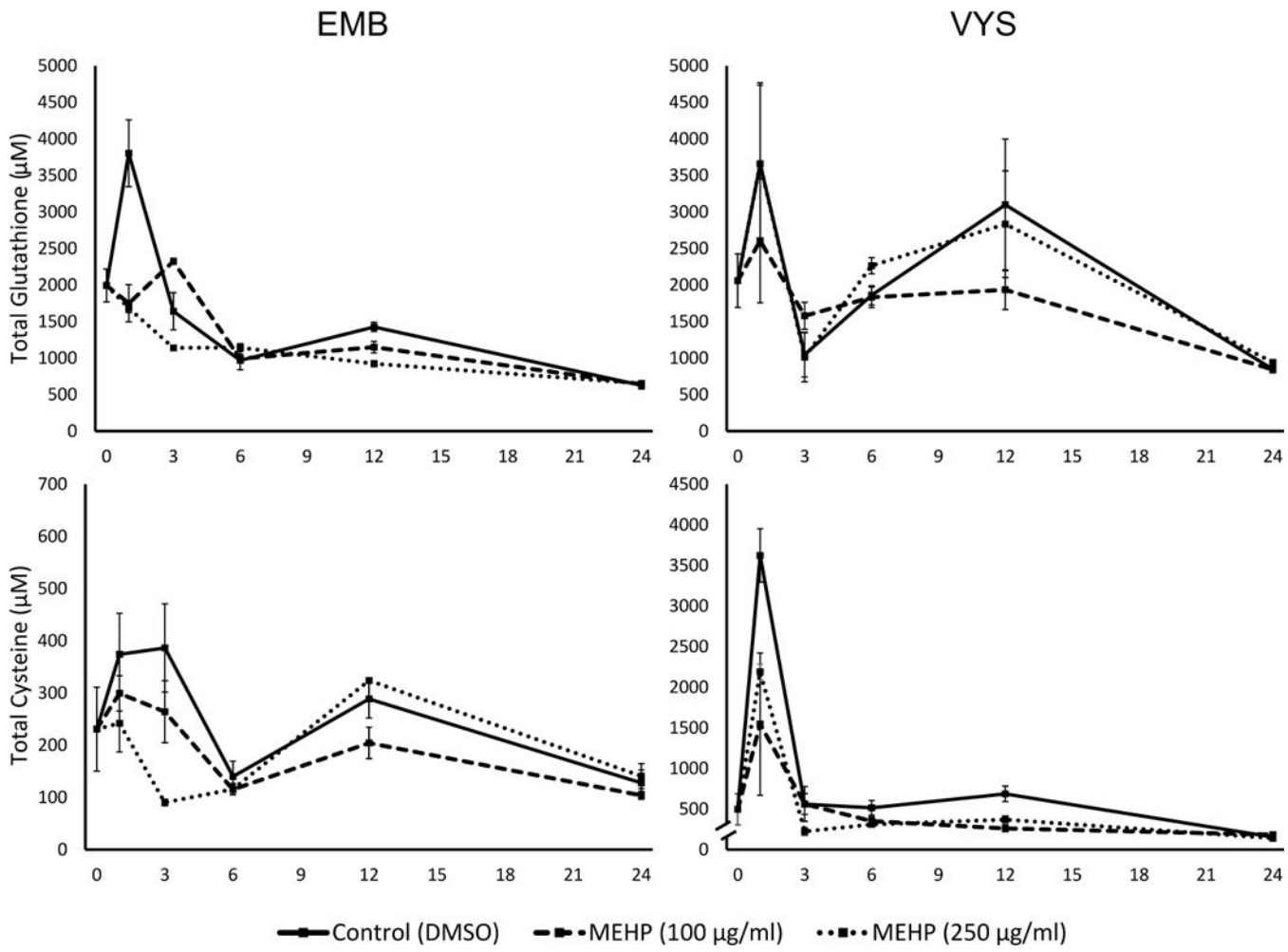

Figure 6.

Ontogeny of total thiol measurements in EMB and VYS following MEHP treatment on GD 8–9. Total concentrations are equal to the sum of the reduced and 2x the oxidized fractions of the thiol, since disulfides were measured. Top left: total glutathione concentrations measured in EM; top right: total glutathione concentrations measured in VYS; Bottom left: total cysteine concentrations measured in EMB; and bottom right: total cysteine concentrations measured in VYS.

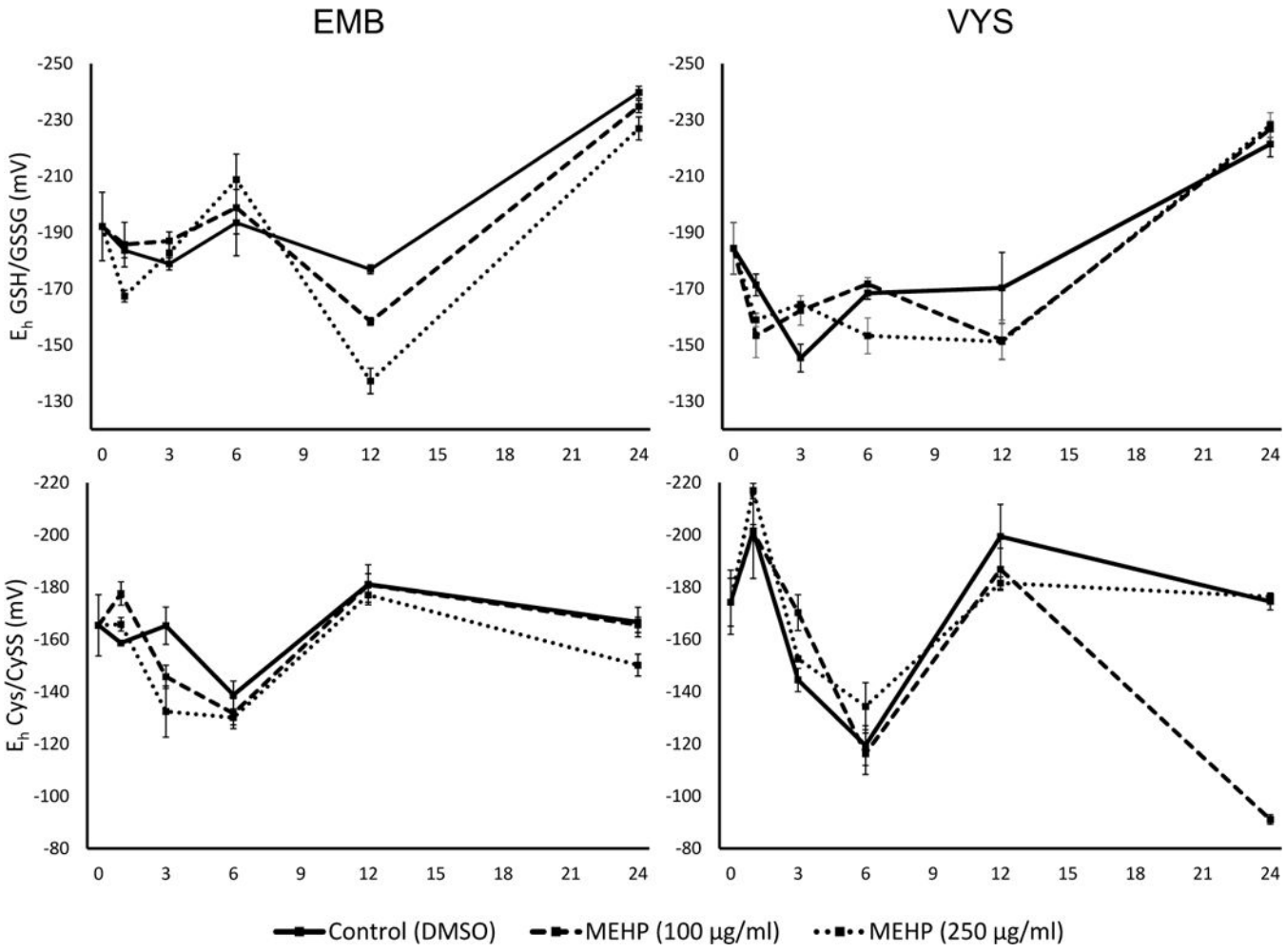

Figure 7.

Ontogenies of redox profiles in conceptal tissues following treatment MEHP treatment on GD8–9. Embryonic redox profiles for glutathione (top left) and cysteine (bottom left) redox couples are shown, as well as VYS redox profiles for glutathione (top right) and cysteine (bottom right) redox couples.

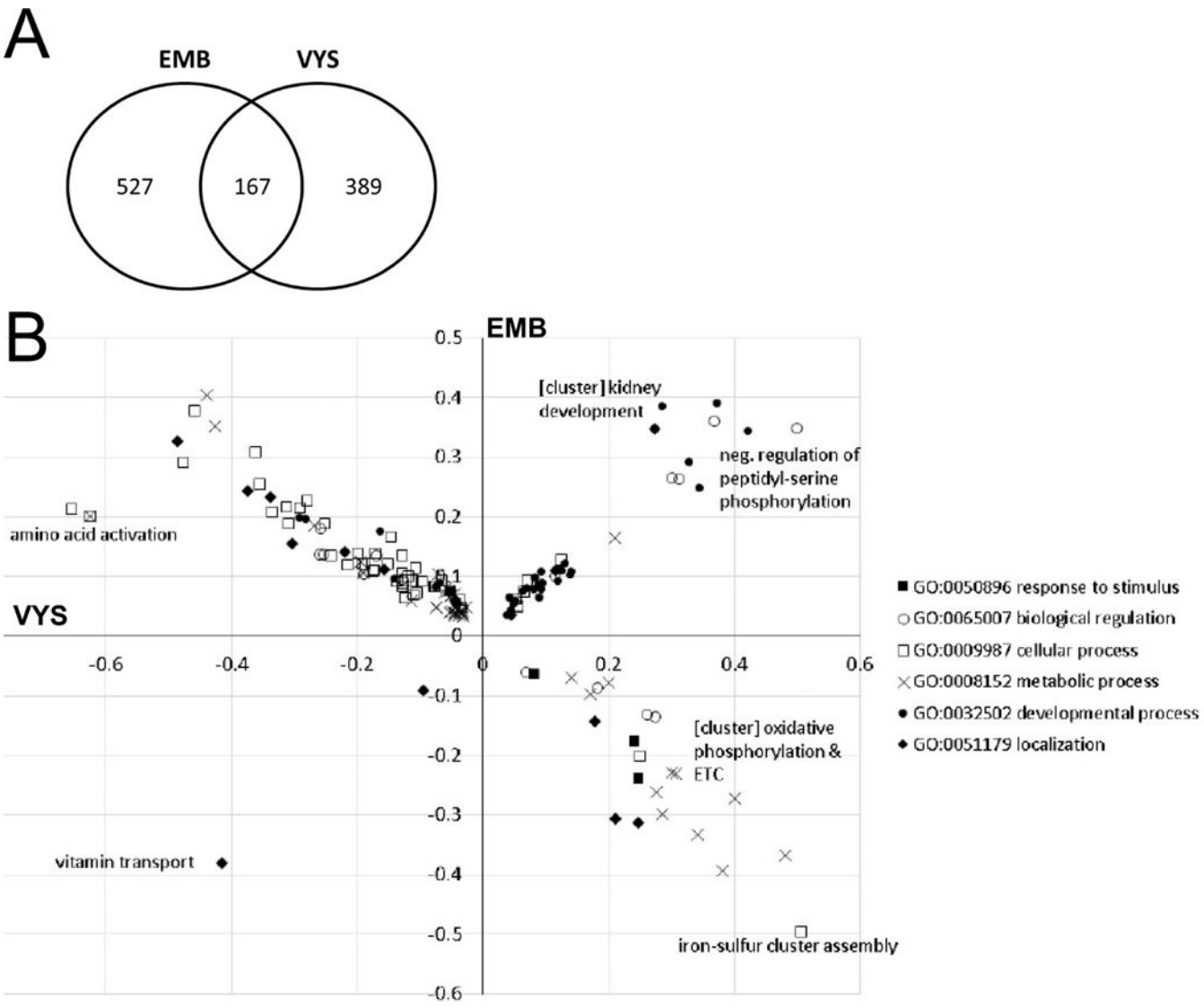

Figure 8.

GO Biological Processes significantly affected by MEHP treatment in both the EMB and VYS. (A) The number of GO Biological Processes significantly altered by MEHP treatment ($p<0.05$) in the EMB, VYS, and both tissues. (B) A plot of direction and magnitude of change (log fold change) of GO Biological Processes significantly affected by MEHP treatment in both the EMB and VYS. Direction and magnitude of process change in the VYS is shown on the x-axis, and for the EMB on the y-axis. Processes, or clusters of related processes, which had high degrees of change due to MEHP treatment in both the EMB and VYS are labeled on the graph.

Table 1

MEHP treatment significantly alters developmental progress in WEC. Though DEHP treatment produced little change in most measurable developmental parameters, the metabolite MEHP significantly altered many defect scores. Values presented are the means ± standard error of the mean. *p<0.05, **p<0.01, ***p<0.001, — indicates that the specimens were too necrotic to accurately assess this parameter.

	Control	MEHP (100 μg/ml)	MEHP (250 μg/ml)	MEHP (500 μg/ml)	MEHP (1 mg/ml)
n	**17**	**7**	**6**	**16**	**5**
Yolk Sac	5.0 ± 0	4.6 ± 0.3	5.0 ± 0	2.1 ± 0.3	0.4 ± 0.2
Allantois	3.0 ± 0	2.6 ± 0.2	3.0 ± 0	1.8 ± 0.2	1.2 ± 0.4
Flexion	4.7 ± 0.1	3.9 ± 0.4	4.3 ± 0.2	4.0 ± 0.1	4.0 ± 0
Heart	3.8 ± 0.1	3.7 ± 0.2	3.5 ± 0.2	3.3 ± 0.1	2.6 ± 0.2
Caudal Neural Tube	4.2 ± 0.1	3.7 ± 0.2	4.0 ± 0	1.3 ± 0.5	–
Hindbrain	4.9 ± 0.1	3.6 ± 0.4	2.8 ± 0.3	3.0 ± 0.3	2.0 ± 0
Midbrain	4.9 ± 0.1	3.6 ± 0.5	2.8 ± 0.4	2.6 ± 0.3	2.0 ± 0
Forebrain	4.6 ± 0.2	3.3 ± 0.5	2.8 ± 0.5	2.9 ± 0.2	2.2 ± 0.2
Otic Vesicle	4.5 ± 0.2	3.3 ± 0.3	2.5 ± 0.2	2.7 ± 0.3	2.4 ± 0.2
Optic Cup	4.6 ± 0.2	3.7 ± 0.4	2.8 ± 0.5	1.9 ± 0.3	1.0 ± 0
Branchial	2.7 ± 0.1	2.6 ± 0.2	2.7 ± 0.2	2.0 ± 0.1	2.0 ± 0
Maxillary	3.0 ± 0	1.9 ± 0.1	2.0 ± 0.1	1.7 ± 0.1	1.0 ± 0
Mandible	2.0 ± 0	2.0 ± 0.2	2.0 ± 0	1.9 ± 0.1	2.0 ± 0
Forelimbs	2.1 ± 0.2	1.9 ± 0.3	2.2 ± 0.2	2.0 ± 0.2	1.6 ± 0.2
Somites (# pairs)	24.6 ± 0.4	21.0 ± 0.8	23.7 ± 0.8	18.8 ± 1.5	—
VYS volume (μl^3)	17.9 ± 1.4	13.8 ± 1.4	17.1 ± 0.8	13.8 ± 1.1	10.2 ± 0.9
Crown-Rump Length (mm)	2.9 ± 0.1	2.7 ± 0.1	2.9 ± 0.1	2.5 ± 0.1	1.7 ± 0.2
Head Length (mm)	1.5 ± 0	1.2 ± 0.1	1.4 ± 0.1	1.2 ± 0	1.0 ± 0.1
TOTAL SCORE	86.6 ± 1.5	73.8 ± 3.8	72.9 ± 2.9	56.6 ± 3.3	28.4 ± 0.8

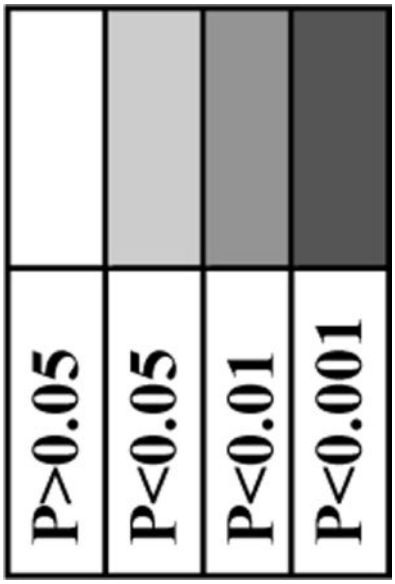

Table 2

EMB and VYS pathways with significantly altered gene expression by 6h MEHP treatment in WEC. Significantly enriched KEGG pathways in the EMB (shown left) and the VYS (shown right) include many metabolic pathways, including severaldependent upon the redox environment, and pathways associated with the nervous system.

Pathways significantly enriched in EMB tissue	Odds Ratio	P-value	Pathways significantly enriched in VYS tissue	Odds Ratio	P-value
Oxidative phosphorylation	4.136	0.001	Oxidative phosphorylation	8.109	0.000
Alanine, aspartate and glutamate metabolism	8.517	0.002	Parkinson’s disease	7.795	0.000
Retinol metabolism	5.637	0.005	Glutathione metabolism	13.522	0.000
Phagosome	3.060	0.008	Alzheimer’s disease	5.166	0.000
Proteasome	5.231	0.010	Aminoacyl-tRNA biosynthesis	11.307	0.000
Rheumatoid arthritis	3.816	0.011	Histidine metabolism	11.235	0.002
Collecting duct acid secretion	6.880	0.012	N-Glycan biosynthesis	8.051	0.002
Purine metabolism	2.679	0.014	Antigen processing and presentation	7.024	0.003
Arginine and proline metabolism	4.135	0.023	Drug metabolism - cytochrome P450	6.644	0.004
Vasopressin-regulated water reabsorption	4.610	0.024	Selenocompound metabolism	14.129	0.006
Starch and sucrose metabolism	4.713	0.028	Huntington’s disease	3.321	0.007
Histidine metabolism	5.117	0.040	Alanine, aspartate and glutamate metabolism	8.852	0.007
Parkinson’s disease	2.633	0.047	Arginine and proline metabolism	5.335	0.015
			Ribosome biogenesis in eukaryotes	4.276	0.022
			Complement and coagulation cascades	3.972	0.039

Table 3

Solute carrier (SLC) family gene expression is significantly impacted by 6h MEHP treatment in WEC. The mitochondrial transport family (SLC25) represents the most significantly altered family of transporters, crucial for the catabolic processes of the cell.

		# genes sig. changed		
SLC family	**Function**	**EMB**	**VYS**	**TOTAL**
1	glial high affinity glutamate/neutral amino acid transporter	1	2	3
4	bicarbonate transporters	6	2	8
5	inositol/sodium-dependent glucose transporters	2	1	3
6	neurotransmitter transporters	3	0	3
7	cationic/L-type amino acid transporters	3	2	5
8	sodium/calcium exchangers	1	1	2
9	sodium/hydrogen exchangers	3	3	6
10	sodium/bile salt exchangers	0	1	1
11	proton-coupled divalent metal ion transporters	1	0	1
12	electroneutral cation-coupled chloride cotransporters	2	1	3
13	sodium sulphate/carboxylate exchangers	0	1	1
16	monocarboxylic acid transporters	6	2	8
17	phosphate/organic anion transporters	2	1	3
19	folate/thiamine transporters	1	1	2
21	organic anion transporters	4	3	7
22	organic cation/anion transporters	4	0	4
23	ascorbate/nucleobase transporters	1	1	2
24	sodium/potassium/calcium exchangers	1	0	1
25	mitochondrial transporters	9	6	15
26	sulfate/anion transporters	2	2	4
29	nucleoside transporters	1	0	1
30	zinc transporters	2	2	4
31	copper transporters	1	0	1
33	acetyl-CoA transporters	0	1	1
35	nucleotide sugar transporters	8	1	9
36	proton-coupled amino acid transporters	0	1	1
37	sugar phosphate exchangers	1	0	1
38	sodium-amino acid cotransporters	1	0	1
39	zinc/metal ion transporters	1	3	4
44	choline transporter-like family	1	2	3
45	putative sugar transporters	2	1	3
46	folate transporters	1	1	2